

# Biosynthetic Incorporation of Site-Specific Isotopes in $\beta$ -Lactam Antibiotics Enables Biophysical Studies

Jacek Kozuch,<sup>‡</sup> Samuel H. Schneider,<sup>‡</sup> and Steven G. Boxer<sup>\*</sup>

Department of Chemistry, Stanford University, Stanford, CA, 94305-5012, USA

E-mail: [sboxer@stanford.edu](mailto:sboxer@stanford.edu)

<sup>‡</sup> These authors contributed equally to this work.

**Abstract:** A biophysical understanding of the mechanistic, chemical, and physical origins underlying antibiotic action and resistance is vital to the discovery of novel therapeutics and the development of strategies to combat the growing emergence of antibiotic resistance. The site-specific introduction of stable-isotope labels into chemically complex natural products is particularly important for techniques such as NMR, IR, mass spectrometry, imaging, and kinetic isotope effects. Towards this goal, we developed a biosynthetic strategy for the site-specific incorporation of  $^{13}\text{C}$ -labels into the canonical  $\beta$ -lactam carbonyl of penicillin G and cefotaxime, the latter via cephalosporin C. This was achieved through sulfur-replacement with 1- $^{13}\text{C}$ -L-cysteine, resulting in high isotope incorporations and mg-scale yields. Using  $^{13}\text{C}$  NMR and isotope-edited IR difference spectroscopy, we illustrate how these molecules can be used to interrogate interactions with their protein targets, e.g. TEM-1  $\beta$ -lactamase. This method provides a feasible route to isotopically-labeled penicillin and cephalosporin precursors for future biophysical studies.

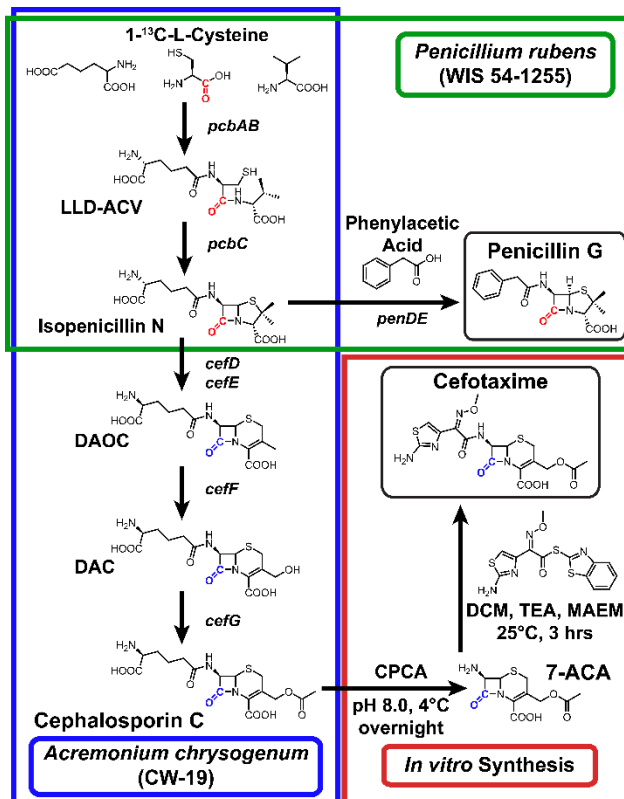
The discovery of penicillin in 1928 by Alexander Fleming marked the beginning of the “antibiotic era”, spurring further discoveries of antibiotic-producing fungi, which revolutionized modern medicine and saved countless lives from the fatal consequences of bacterial infections.<sup>[1]</sup> However, the increasing (mis)use of antibiotics has resulted in the emergence of multi- and super-resistant bacteria, such as MRSA (methicillin-resistant *Staphylococcus aureus*) or the New Delhi metallo- $\beta$ -lactamase containing *K. pneumonia*, which present major global health threats.<sup>[2-3]</sup> A biophysical understanding of the mechanistic, chemical, and physical origins underlying antibiotic action and resistance is therefore vital to the discovery of novel therapeutics and the development of strategies to combat the growing emergence of antibiotic resistance.<sup>[4]</sup> Biophysical studies can provide highly specific structural, functional, and/or dynamic information using analytical techniques such as infrared (IR) spectroscopy,<sup>[5-7]</sup> nuclear magnetic resonance (NMR),<sup>[8-9]</sup> mass spectrometry (MS),<sup>[9-11]</sup> imaging,<sup>[12]</sup> kinetic isotope effects (KIE's),<sup>[13-14]</sup> etc. However, many of these approaches require (or at least benefit from) the site-specific introduction of stable isotopes into biologically relevant molecules. While chemical synthesis can provide a general route for isotopic incorporation in small molecules,<sup>[15-16]</sup> there are many complex biomolecules such as  $\beta$ -lactam antibiotics where the presence of multiple functional groups and stereocenters renders (semi-)biosynthesis a more elegant, efficient, cost-effective, and sometimes even necessary approach.

$\beta$ -Lactam antibiotics are the most widely used antibiotic agents.<sup>[17]</sup> Their medical importance has inspired many heroic studies in both chemical<sup>[18-19]</sup> and biosynthetic approaches, but the latter proved more economically efficient, and thus became the nearly exclusive route to  $\beta$ -lactam

antibiotics and their precursors. This has led to development of chemically-defined media formulations in order to elucidate the metabolic precursors to  $\beta$ -lactams, engineer existing biosynthetic pathways, and improve antibiotic scope and yields in  $\beta$ -lactam producing fungi.<sup>[20-24]</sup> There are, however, no commercially available penicillin or cephalosporin derivatives with site-specific isotope labels on the  $\beta$ -lactam core (several are available with isotopes on the chemically-introduced side-chain). Such isotopic labels would be of particular interest as they could be used to monitor changes at or in close vicinity to the functional center of the antibiotic during both covalent (e.g. inhibition of transpeptidases, and acyl-enzyme intermediate of  $\beta$ -lactamases) and non-covalent interactions (e.g. binding in efflux pumps such as AcrB<sup>[25]</sup>) as well as antibiotic turnover, in an antibiotic-dependent manner without perturbative labels or chemical modification.<sup>[26]</sup> There have been previous studies where isotopic labels were introduced biosynthetically at specific positions to penicillins, mainly to characterize the mechanism of penicillin synthesis and assign the chemical origin of the bicyclic  $\beta$ -lactam structure.<sup>[27-30]</sup> However, the labeled penicillins were not produced and isolated at preparative scales that would be useful for biophysical studies. Since both aspects are essential requirements for the aforementioned biophysical studies, we present in this work a complete protocol for the site-specific introduction of a  $^{13}\text{C}$  isotope into the  $\beta$ -lactam carbonyl group of penicillin G (PenG) and the cephalosporin, cefotaxime (CTX), and their production and isolation at mg scale. We refer to these molecules throughout as  $^{13}\text{C}_{\text{CO}}$ -PenG and  $^{13}\text{C}_{\text{CO}}$ -CTX, respectively, where the subscript denotes the desired site-specific labeling at the C=O of the  $\beta$ -lactam.

As shown in Scheme 1 and extensively reviewed in the literature,<sup>[31]</sup> PenG can be obtained directly as a metabolic product of *Penicillium* strains (green box) through utilization of three amino acid building blocks, L-aminoadipic acid, L-cysteine, and L-valine, in addition to the presence of N-terminal side-chain precursors, such as phenylacetic acid. While cephalosporin biosynthesis relies on the same three amino acids (blue box), there are no direct *in situ* routes to commercially and medically relevant antibiotics, such as CTX and ceftazidime, thus requiring further (bio)chemical processing. As a consequence, final metabolites such as cephalosporin C (CPC) are isolated and converted enzymatically and/or chemically to the desired antibiotic (red box). As the biosynthesis of both  $\beta$ -lactam antibiotics proceeds through common intermediates, i.e. the LLD-ACV tripeptide and isopenicillin V, in which the  $\beta$ -lactam carbonyl group originates from cysteine's carboxylate group (red or blue colored C=O group in Scheme 1), we sought a method for utilizing cysteine as the exclusive sulfur source in chemically defined media. Yeasts and filamentous fungi produce cysteine through the autotrophic and/or transsulfuration pathways, whereby sulfur is obtained from inorganic sulfate in the former and methionine via S-adenosylmethionine in the latter.<sup>[24, 32-34]</sup> Therefore, we reasoned that replacement of all inorganic sulfate and sulfur-containing biomolecules and feedstocks with L-cysteine (and/or DL-methionine) might be expected to (at least partially) suppress the endogenous cysteine biosynthesis in favor of uptake of externally provided amino acids and their utilization in both primary and secondary metabolic pathways, thereby removing the need for auxotrophic fungal strains. Based on this general approach, we modified chemically defined media to utilize L-cysteine (and DL-methionine for CTX) as exclusive sulfur sources in order to bias the isotopic incorporation. Herein, we refer to all sulfur-modified media formulations where the sulfate has been removed and replaced with L-cysteine and/or DL-methionine with "(S)" after the media name. In this way, we introduced site-specific  $^{13}\text{C}$  isotope labels to the  $\beta$ -lactam carbonyls of PenG and CTX (via CPC) through

biosynthetic production in low-to-moderate antibiotic-producing progenitor fungal strains available from the American Type Culture Collection (ATCC), *Penicillium rubens* (WIS 54-1255) and *Acremonium chrysogenum* (CW-19), respectively.



**Scheme 1.** Synthetic pathway to penicillin G and cefotaxime. Biosynthetic production of penicillin G by *Penicillium rubens* (WIS 54-1255) (green box) and cephalosporin C by *Acremonium chrysogenum* (CW-19) (blue box), which can be converted in vitro to cefotaxime (red box). The position of the site-specific <sup>13</sup>C carbonyl (C=O) label is indicated in red and blue for PenG and CTX, respectively.

For the <sup>13</sup>C<sub>CO</sub>-PenG production, we utilized chemically defined media formulations based on work from Driessen and Martin, i.e. PPM and MDFP, respectively,<sup>[35-36]</sup> with the WIS 54-1255 strain. We monitored the excreted PenG via HPLC for both PPM(S) and MDFP(S) (Figure 1A), and observed minimal PenG in the former and ca. 0.1 – 0.2 mg mL<sup>-1</sup> in the latter, presumably due to strain-specific media optimization.<sup>[37]</sup> In an attempt to improve yields we augmented the PPM(S) medium with ethylamine and citric acid, which are used under MDFP conditions. We denote this modified PPM media formulation as “PPM+” and “PPM+(S)” (Table S1) and were able to increase the PenG production by a factor of 3 – 4 relative to MDFP(S). Furthermore, based on daily HPLC monitoring we determined the optimal time point of PenG isolation to be after 6 – 8 days of production, with a total yield of 0.4 – 0.6 mg mL<sup>-1</sup> (Figure 1B). Interestingly, a change of the pH of the growth medium from 6.3 to ca. 8 – 8.5 during days 6 – 8 coincided with increasing and maximal PenG yield, so that the pH can thus be used as a simple way to monitor PenG production.<sup>[38]</sup> The antibiotic was isolated and purified by removal of the fungal cell mass using filtration and

lyophilization to obtain the dry mass of the excreted media and purified further with HPLC on a preparative reversed-phase C18 column. The incorporation of 1-<sup>13</sup>C-L-cysteine from sulfate-depleted PPM+(S) medium into PenG was confirmed using MS analysis (Figure 1E), which provided the expected molecular mass of 333.92 Da (in ESI- mode) corresponding to the [<sup>13</sup>C<sub>CO</sub>-PenG - H]<sup>+</sup> species. No detectable masses at 333 or at higher masses indicating multiple <sup>13</sup>C incorporations were observed in the MS data, indicating an incorporation of >95% for a single <sup>13</sup>C isotope (see below for assignment of site-specificity).

In order to obtain <sup>13</sup>C-labeled CPC (<sup>13</sup>C<sub>CO</sub>-CPC), the precursor to current cephalosporin antibiotics, we modified the previously reported chemically-defined DFM medium from Demain and colleagues analogously to the sulfur-depletion strategy for PenG, referred to as DFM(S) media (Table S2).<sup>[39]</sup> Unlike PenG, monitoring the concentration of CPC via the corresponding HPLC elution peak at ca. 23.5 min (Figure 1C) is more difficult due to the crowded nature of this elution region and potential overlap with other metabolites and CPC precursors. Therefore, we used the intensity of this elution peak as a proxy for the CPC amount and determined that a maximum concentration is reached after ca. 15 days (Figure 1D). Analogous to that observed with PenG and WIS 54-1255, the pH follows the growth of CPC production until a coincident maximum is observed. The longer production times to enrich the medium with CPC can be understood based on the more complex biosynthesis and corresponding enzymatic steps (Scheme 1, blue box), each of which has been extensively studied.<sup>[39-42]</sup> Interpolating from the finally isolated CTX, the concentration of CPC plateaus at ca. 0.010 – 0.060 mg mL<sup>-1</sup> using the DFM(S) growth medium. This considerably lower yield can be ascribed to the slower growths and complexity of the sulfur metabolism in *Acremonium* (SI section 3.3).<sup>[24]</sup> CPC was isolated analogously to PenG and subsequently subjected to enzymatic cleavage of the aminoadipic side-chain using a mutant of cephalosporin C acylase (CPCA) from *Pseudomonas* sp. in order to obtain the medically-relevant cephalosporin precursor 7-aminocephalosporanic acid, 7-ACA (Scheme 1, Figure 1C). This reaction showed close to stoichiometric conversion of CPC to 7-ACA (26.5 min), enabling purification due to the retention of co-purified metabolites at 23.5 min in HPLC. In the final step, 7-ACA was reacted with the 2-mercaptobenzothiazolyl thioester of (*Z*)-2-[2-aminothiazol-4-yl]-2-methoxyimino acetic acid (MAEM) in dichloromethane (3h, RT)<sup>[43]</sup> to yield CTX (0.011 – 0.066 mg mL<sup>-1</sup>; purified via HPLC) (Figure 1C). In this case, the addition of 1-<sup>13</sup>C-L-cysteine, both with and without 1-<sup>13</sup>C-DL-methionine, to sulfur-depleted media resulted in ca. 50% isotope incorporation of only a single <sup>13</sup>C-label as evidenced by two main molecular peaks with a mass difference of ca. ±1 in the MS data of CPC and CTX (Figure 1F,G).

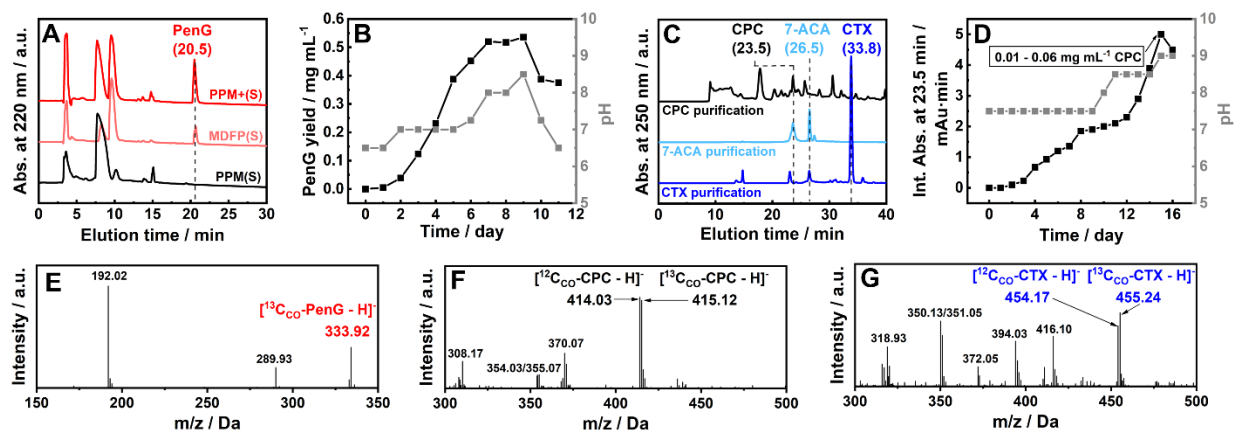


**Figure 1.** Biosynthetic production of  $^{13}\text{C}_{\text{co}}$ -PenG and  $^{13}\text{C}_{\text{co}}$ -CTX (via  $^{13}\text{C}_{\text{co}}$ -CPC and  $^{13}\text{C}_{\text{co}}$ -7-ACA). A,C: HPLC chromatograms of the production of (A) PenG (20.5 min, analytical C18 column) in different sulfur-depleted but  $1\text{-}^{13}\text{C}$ -L-cysteine-enriched media, and of (C) the isolated CPC (23.5 min; black trace) in DFM(S) media as well as the purified 7-ACA (26.5 min; light blue) and CTX (33.8 min; blue trace; all preparative C18 column). Offset for clarity. B,D: Time-dependent production of (B) PenG using WIS 54-1255 in PPM+(S) media and of (D) CPC using CW-19 in DFM(S) media with maximum CPC yield of ca.  $0.01 - 0.06 \text{ mg mL}^{-1}$ . Corresponding pH changes in both cases are shown in grey. E,F,G: Mass spectra of  $^{13}\text{C}_{\text{co}}$ -PenG,  $^{13}\text{C}_{\text{co}}$ -CPC and  $^{13}\text{C}_{\text{co}}$ -CTX in ESI- mode, with the molecular (-H) peak highlighted in red, black and blue, respectively. For  $^{13}\text{C}_{\text{co}}$ -PenG > 95%  $^{13}\text{C}$  incorporation is observed; for  $^{13}\text{C}_{\text{co}}$ -CPC and  $^{13}\text{C}_{\text{co}}$ -CTX two molecular (-H) peaks with masses of  $\pm 1 \text{ Da}$  and similar intensities indicate an approximate  $^{13}\text{C}_{\text{co}}$  incorporation yield of 50 %.

Further confirmation that the  $^{13}\text{C}$ -label is introduced into the  $\beta$ -lactam C=O can be observed from comparison of the MS fragmentation patterns between  $^{12}\text{C}$ - and  $^{13}\text{C}$ -containing  $\beta$ -lactams. Primarily, it is observed that the dominant fragments that contain a +1 Da mass are originating from the bicyclic  $\beta$ -lactam core (SI section 2.5 and 3.6). Furthermore, utilizing Fourier-transform infrared (FTIR) spectroscopy we observe that the characteristic high-frequency  $\beta$ -lactam carbonyl stretching frequency ( $\nu_{\text{C=O}}$ ) is shifted in the corresponding  $^{12}\text{C}_{\text{co}}$  and  $^{13}\text{C}_{\text{co}}$  molecules (Figure 2A,B). As a consequence, the isotope-edited difference spectra ( $^{12}\text{C}_{\text{co}} - ^{13}\text{C}_{\text{co}}$ ) exhibits only a single peak that changes in the spectral window of carbonyls, with a frequency shift ( $\Delta\nu = \nu_{^{12}\text{C=O}} - \nu_{^{13}\text{C=O}}$ ) of ca.  $45 \text{ cm}^{-1}$  for both penicillin G and cefotaxime. These results are in agreement with the assignments and frequencies from density functional theory (DFT) frequency calculations of the  $^{12}\text{C}_{\text{co}}$  and  $^{13}\text{C}_{\text{co}}$  biomolecules (SI section 5.1). Taken together, the LC-MS, FTIR, and DFT results unambiguously verify the site-specific introduction of a single  $^{13}\text{C}$ -label at the  $\beta$ -lactam C=O ( $^{13}\text{C}_{\text{co}}$ ).

The incorporation of site-specific isotopes enables experiments that were not previously possible, such as NMR, MS, and IR spectroscopy. To illustrate the usefulness of these new species, we measured the FTIR and NMR spectra of PenG in complex with the deacylation-impaired mutant (E166N) of TEM-1  $\beta$ -lactamase, leading to a covalent acyl-enzyme adduct.<sup>[44]</sup> As previously shown, the IR frequency and  $^{13}\text{C}$  NMR chemical shift of carbonyls are sensitive to their local, site-specific chemical environment, primarily through electrostatic interactions.<sup>[45-47]</sup> The 1D  $^{13}\text{C}$  NMR spectrum of  $^{13}\text{C}_{\text{co}}$ -PenG in buffer exhibits a single sharp peak at 177.3 ppm which is broadened and shifted downfield to 179.8 ppm in the acyl-enzyme of  $^{13}\text{C}_{\text{co}}$ -PenG-TEM-1 (Figure

2C). Besides demonstrating the formation of the covalent complex, the downfield shift can hold information about the strength of intermolecular interactions within the enzyme active site.<sup>[45, 48]</sup> In addition, FTIR difference spectroscopy can provide analogous information about the chemical environment within the protein active site.<sup>[49]</sup> As shown in Figure 2A, the isotope-edited FTIR difference spectra ( $^{12}\text{C}_{\text{CO}} - ^{13}\text{C}_{\text{CO}}$ ) of PenG provides a characteristic ‘fingerprint’, i.e. a positive and negative peak with a frequency offset ( $\Delta\nu \sim 45 \text{ cm}^{-1}$ ), which can be used for spectroscopic assignment and monitoring of the functional  $\beta$ -lactam C=O. Utilizing this isotopic shift, we measured the difference spectrum of the  $^{12}\text{C}_{\text{CO}}$ -PenG-TEM-1 and  $^{13}\text{C}_{\text{CO}}$ -PenG-TEM-1 acyl-enzyme complexes (Figure 2D). Noticeably, we observe a series of alternating positive ( $^{12}\text{C}_{\text{CO}}$ ) and negative ( $^{13}\text{C}_{\text{CO}}$ ) peaks, with a frequency offset between pairs of peaks consistent with those observed in Figure 2A, but with much narrower linewidths and at significantly lower frequency compared to the  $\beta$ -lactam C=O in deuterated buffer. Note that the linewidths for carbonyl groups in proteins are typically much narrower than those in water, which can be partially attributed to the differences in inhomogeneous broadening due to the environment.<sup>[46, 50]</sup> The observation of multiple sets of C=O peaks is indicative of distinct conformations of the covalent PenG adduct in the enzyme active site, which was suggested previously, but could not be confirmed in the absence of isotopic labeling.<sup>[5-7, 51]</sup> Taking into account the different timescales of the NMR and FTIR measurements and noting the single peak in the 1D  $^{13}\text{C}$  NMR spectrum, this indicates an exchange of the conformational species on the sub-ms to ps time scale (the homogeneous lifetime of most C=O vibrations is ca. 1-5 ps).<sup>[52]</sup> These isotopic probes and difference spectroscopy enables further investigations in complex environments such as  $\beta$ -lactamases and transpeptidases, thereby providing new insights into antibiotic action and resistance<sup>[5-6]</sup>, which will be reported separately.

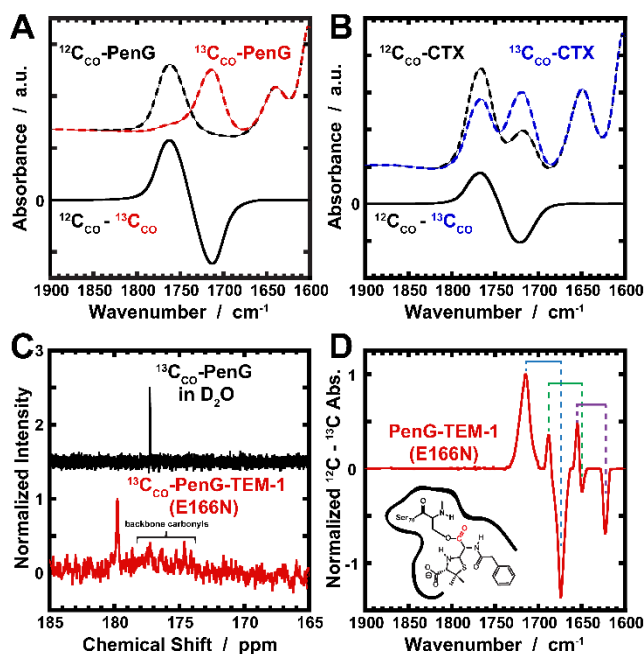


**Figure 2.** Isotope-enabled spectroscopic characterization and applications in TEM-1  $\beta$ -Lactamase. FTIR spectra of  $^{12}\text{C}_{\text{CO}}$  and  $^{13}\text{C}_{\text{CO}}$   $\beta$ -lactams, (A) penicillin G (black and red dashed lines, respectively) and (B) cefotaxime (black and blue dashed lines, respectively) and corresponding isotope difference spectra ( $^{12}\text{C}_{\text{CO}}$

–  $^{13}\text{C}_{\text{CO}}$ ; solid black line) in deuterated aqueous buffer (50 mM  $\text{KPi}$ , 100 mM  $\text{NaCl}$ , pH 7.0), offset for clarity. C: 1D  $^{13}\text{C}$  NMR of  $^{13}\text{C}_{\text{CO}}$ -penicillin G in  $\text{D}_2\text{O}$  buffer (black) and TEM-1 E166N (red). D: FTIR isotope-edited difference spectrum of TEM-1 E166N  $\beta$ -lactamase in the acyl-enzyme complex (see inset diagram) with penicillin G. Color-coded brackets indicate corresponding pairs of  $^{12}\text{C}$  (positive) and  $^{13}\text{C}$  (negative) peaks.

In conclusion, utilization of sulfur-depleted chemically-defined media enabled site-specific  $^{13}\text{C}_{\text{CO}}$  isotope incorporation in PenG and CTX at the mg scale (per 50 mL of growth medium), which can be conveniently scaled for higher absolute yields for biophysical studies. This biosynthetic route further enables a feasible route to 6-APA, the precursor to all semi-synthetic penicillin derivatives, through cleavage of the phenylacetic (or phenoxyacetic acid in penicillin V) side-chain using commercially available enzymes, e.g. penicillin amidase (E.C. 3.5.1.11), analogous to the process undergone with conversion of CPC to CTX. This method for introduction of site-specific isotope labels in complex biomolecules, such as the canonical penicillin and cephalosporin  $\beta$ -lactams, enables new biophysical investigations that have not been previously possible, as demonstrated with NMR and FTIR spectroscopy in TEM-1  $\beta$ -lactamase, to better understand antibiotic resistance.

## Acknowledgements

We would like to thank the lab of Arnold J. M. Driessen at the University of Groningen, especially Riccardo Iacovelli and László Mózsik, as well as the lab of Elizabeth Sattely at Stanford University, especially Amy Calgaro-Kozina. We appreciate strain recommendations for CPC production from Arnold Demain at Drew University. We would also like to acknowledge the Vincent Coates Foundation Mass Spectrometry Laboratory at Stanford University and Stephen Lynch for support with NMR. J.K. acknowledges the Deutsche Forschungsgemeinschaft for a Research Fellowship (KO5464/1). This work is supported by NIH Grant GM118044 (to S.G.B.).

## References:

- [1] C. C. Muñiz, T. E. C. Zelaya, G. R. Esquivel, F. J. Fernández, *Rev. Latinoam. Microbiol.* **2007**, 49, 88-98.
- [2] B. Chandar, S. Pati, D. Bhattacharya, *J. Antimicrob. Agents* **2018**, 04.
- [3] S. Harbarth, H. H. Balkhy, H. Goossens, V. Jarlier, J. Kluytmans, R. Laxminarayan, M. Saam, A. Van Belkum, D. Pittet, and for the World Healthcare-Associated Infections Resistance Forum participants, *Antimicrob. Resist. Infect. Control* **2015**, 4, 49-63.
- [4] J. R. Knowles, *Acc. Chem. Res.* **1985**, 18, 97-104.
- [5] A.-S. Wilkinson, W. Simon, M. Kania, M. G. P. Page, C. W. Wharton, *Biochemistry* **1999**, 38, 3851-3856.
- [6] A.-S. Wilkinson, P. K. Bryant, S. O. Meroueh, M. G. P. Page, S. Mobashery, C. W. Wharton, *Biochemistry* **2003**, 42, 1950-1957.
- [7] J. Fisher, J. G. Belasco, S. Khosla, J. R. Knowles, *Biochemistry* **1980**, 19, 2895-2901.
- [8] K. A. Manning, B. Sathyamoorthy, A. Eletsky, T. Szyperki, A. S. Murkin, *J. Am. Chem. Soc.* **2012**, 134, 20589-20592.
- [9] D. E. Ehmann, H. Jahić, P. L. Ross, R. F. Gu, J. Hu, T. F. Durand-Réville, S. Lahiri, J. Thresher, S. Livchak, N. Gao, T. Palmer, G. K. Walkup, S. L. Fisher, *J. Biol. Chem.* **2013**, 288, 27960-27971.

- [10] J. E. Hugonnet, D. Mengin-Lecreux, A. Monton, T. den Blaauwen, E. Carbonnelle, C. Veckerlé, Y. V. Brun, M. van Nieuwenhze, C. Bouchier, K. Tu, L. B. Rice, M. Arthur, *Elife* **2016**, 5.
- [11] M. M. Lozano, J. S. Hovis, F. R. Moss, 3rd, S. G. Boxer, *J. Am. Chem. Soc.* **2016**, 138, 9996-10001.
- [12] L. Wei, Z. Chen, L. Shi, R. Long, A. V. Anzalone, L. Zhang, F. Hu, R. Yuste, V. W. Cornish, W. Min, *Nature* **2017**, 544, 465-470.
- [13] Z. Wang, D. Antoniou, S. D. Schwartz, V. L. Schramm, *Biochemistry* **2016**, 55, 157-166.
- [14] W. W. Cleland, *Arch. Biochem. Biophys.* **2005**, 433, 2-12.
- [15] K. C. Nicolaou, D. Vourloumis, N. Winssinger, P. S. Baran, *Angew. Chem. Int. Ed. Engl.* **2000**, 39, 44-122.
- [16] J. R. Hanson, *The Organic Chemistry of Isotopic Labelling*, Royal Society of Chemistry, Cambridge, **2011**.
- [17] K. Bush, P. A. Bradford, *Cold Spring Harb. Perspect. Med.* **2016**, 6, 1-22.
- [18] J. C. Sheehan, K. R. Henery-Logan, *J. Am. Chem. Soc.* **1959**, 81, 3089-3094.
- [19] R. B. Woodward, H. Gosteli, J., P. Naegeli, W. Oppolzer, R. Ramage, S. Ranganathan, H. Vorbrüggen, *J. Am. Chem. Soc.* **1966**, 88, 852-853.
- [20] F. Guzmán-Chávez, R. D. Zwahlen, R. A. L. Bovenberg, A. J. M. Driessen, *Front. Microbiol.* **2018**, 9, 2768.
- [21] C. T. Calam, D. J. D. Hockenhuill, *Microbiology* **1949**, 3, 19-31.
- [22] B. Christensen, Nielsen, Jens, *Biotechnol. Bioeng.* **2000**, 68, 652-659.
- [23] G. Bradfield, P. Somerfield, T. Meyn, M. Holby, D. Babcock, D. Bradley, I. H. Segel, *Plant Physiol.* **1970**, 46, 720-727.
- [24] J. F. Martín, A. L. Demain, *Trends Biotechnol.* **2002**, 20, 502-507.
- [25] A. Atzori, G. Malloci, J. D. Prajapati, A. Basciu, A. Bosin, U. Kleinekathöfer, J. Dreier, A. V. Vargiu, P. Ruggerone, *J. Phys. Chem. B* **2019**, 123, 4625-4635.
- [26] D. G. Brenner, J. R. Knowles, *Biochemistry* **1984**, 23, 5833-5839.
- [27] S. C. Warren, G. G. F. Newton, E. P. Abraham, *Biochem. J.* **1967**, 103, 902-912.
- [28] P. Adriaens, H. Vanderhaeghe, B. Meesschaert, H. Eyssen, *Antimicrob. Agents Chemother.* **1975**, 8, 15-17.
- [29] E. Albu, R. Thomas, *Biochem J.* **1963**, 87, 648-652.
- [30] C. M. Stevens, E. Inamine, C. W. De Long, *J. Biol. Chem.* **1956**, 219, 405-409.
- [31] S. S. Weber, R. A. Bovenberg, A. J. Driessen, *Biotechnol. J.* **2012**, 7, 225-236.
- [32] I. H. Segel, M. J. Johnson, *Arch. Biochem. Biophys.* **1963**, 193, 216-226.
- [33] M. van de Kamp, E. Pizzinini, A. Vos, T. R. van der Linder, T. A. Schuurs, R. W. Newbert, G. Turner, W. N. Konings, A. J. M. Driessen, *J. Bacteriol.* **1999**, 181, 7228-7234.
- [34] P. G. Caltrider, H. F. Niss, *Appl. Environ. Microbiol.* **1966**, 14, 746-753.
- [35] S. S. Weber, F. Polli, R. Boer, R. A. Bovenberg, A. J. Driessen, *Appl. Environ. Microbiol.* **2012**, 78, 7107-7113.
- [36] R. Domínguez-Santos, K. Kosalková, C. García-Estrada, C. Barreiro, A. Ibáñez, A. Morales, J. F. Martín, *J. Proteomics* **2017**, 156, 52-62.
- [37] J. G. Nijland, B. Ebbendorf, M. Woszczynska, R. Boer, R. A. Bovenberg, A. J. Driessen, *Appl. Environ. Microbiol.* **2010**, 76, 7109-7115.
- [38] F. G. Jarvis, M. J. Johnson, *J. Am. Chem. Soc.* **1947**, 69, 3010-3017.
- [39] Y. Shen, S. Wolfe, A. L. Demain, *Nat. Biotechnol.* **1986**, 4, 61-64.
- [40] S. M. Samson, J. E. Dotzla, M. L. Slisz, G. W. Becker, R. M. Van Frank, L. E. Veal, W.-K. Yeh, J. R. Miller, S. W. Queener, T. D. Ingolia, *Nat. Biotechnol.* **1987**, 5, 1207-1214.
- [41] J. Velasco, S. Gutierrez, S. Campoy, J. F. Martín, *Biochem. J.* **1999**, 337, 379-385.
- [42] F. R. Ramos, M. J. López-Nieto, J. F. Martín, *FEMS Microbiol. Lett.* **1986**, 35, 123-127.
- [43] J. C. Rodríguez, R. Hernández, M. González, M. A. López, A. Fini, *Il Farmaco* **2000**, 55, 393-396.



- [44] N. C. J. Strynadka, H. Adachi, S. E. Jensen, K. Johns, A. Sielecki, C. Betzel, K. Sutoh, M. N. G. James, *Nature* **1992**, 359, 700-705.
- [45] S. M. Kashid, S. Bagchi, *J. Phys. Chem. Lett.* **2014**, 5, 3211-3215.
- [46] S. H. Schneider, S. G. Boxer, *J. Phys. Chem. B* **2016**, 120, 9672-9684.
- [47] S. D. Fried, S. G. Boxer, *Acc. Chem. Res.* **2015**, 48, 998-1006.
- [48] A. T. Fafarman, P. A. Sigala, D. Herschlag, S. G. Boxer, *J. Am. Chem. Soc.* **2010**, 132, 12811-12813.
- [49] S. D. Fried, S. G. Boxer, *Annu. Rev. Biochem.* **2017**, 86, 387-415.
- [50] S. H. Schneider, H. T. Kratochvil, M. T. Zanni, S. G. Boxer, *J. Phys. Chem. B* **2017**, 121, 2331-2338.
- [51] G. A. Cortina, J. M. Hays, P. M. Kasson, *ACS Catal.* **2018**, 8, 2741-2747.
- [52] P. Hamm, M. Zanni, *Concepts and Methods of 2D Infrared Spectroscopy*, Cambridge University Press, Cambridge, **2011**.

# Supplementary Information for Biosynthetic Incorporation of Site-Specific Isotopes in $\beta$ -Lactam Antibiotics Enables Biophysical Studies

Jacek Kozuch,<sup>‡</sup> Samuel H. Schneider,<sup>‡</sup> Steven G. Boxer  
*Dept. of Chemistry, Stanford University, Stanford, CA, 94305-5012, USA*

<sup>‡</sup>These authors contributed equally to this work.

## Table of Contents:

1. Materials & Methods
  - 1.1. General Comment and Overview
  - 1.2. Chemicals
  - 1.3. Fungal Strains
  - 1.4. General Information
  - 1.5. Instrumentation and Analysis
2. <sup>13</sup>C<sub>CO</sub>-Incorporation in Penicillin G with *Penicillium rubens* WIS 54-1255
  - 2.1. Solid Media
  - 2.2. Starter Media
  - 2.3. Penicillin Production Media
  - 2.4. Penicillin G Extraction and Purification
  - 2.5. PenG MS Fragmentation: Site-Specific Labeling
3. <sup>13</sup>C<sub>CO</sub>-Incorporation in Cephalosporin C with *Acremonium chrysogenum* CW-19
  - 3.1. Solid Media
  - 3.2. Starter Media
  - 3.3. Cephalosporin C Production Media
  - 3.4. Cephalosporin C Extraction and Purification
  - 3.5. Conversion of CPC to 7-ACA, and 7-ACA to CTX
  - 3.6. CPC and CTX MS Fragmentation: Site-Specific Labeling
4. Cephalosporin C Acylase
  - 4.1. Plasmid construction and sequence of Cephalosporin C Acylase
  - 4.2. Protein sequence of Cephalosporin C Acylase
  - 4.3. Protein expression and purification of Cephalosporin C Acylase
  - 4.4. Reaction monitoring of CPCA activity with UV-vis and HPLC
5. Using site-specific <sup>13</sup>C-labeled PenG and CTX for protein studies
  - 5.1. Assignment of <sup>13</sup>C=O mode of  $\beta$ -lactam using DFT
  - 5.2. Nucleotide Sequence of TEM-1 E166N  $\beta$ -Lactamase
  - 5.3. Protein Sequence of TEM-1 E166N  $\beta$ -Lactamase
  - 5.4. Protein Expression and Purification of TEM-1 E166N  $\beta$ -Lactamase
  - 5.5. FTIR Spectroscopy of PenG and TEM-1 E166N  $\beta$ -Lactamase
  - 5.6. NMR Spectroscopy of PenG and TEM-1 E166N  $\beta$ -Lactamase
6. Appendix: Additional Information
  - 6.1. Penicillin G Production with WIS 54-1255
    - 6.1.1. Solid Media for Sporulation

- 6.1.2. PenG Producing Starter and Production Media Combinations
- 6.1.3. PenG Non-Producing Starter and Production Media Combination
- 6.1.4. <sup>15</sup>N-Incorporation Media Formulation
- 6.1.5. <sup>15</sup>N-Isotopic Enrichment: LC-MS and FTIR spectra
- 6.2. Cephalosporin C Production with CW-19
  - 6.2.1. Solid Media for Sporulation
  - 6.2.2. Isolation of CW-19 from ATCC 36225 Sample for CPC Production
- 7. References

## 1. **Materials & Methods**

### 1.1 ***General Comment and Overview***

While the world production of  $\beta$ -lactams antibiotics and precursors (> 40,000 metric tons as of 2000) can be achieved in fed-batch semi-continuous flow reactors,<sup>[1]</sup> protocols for small (mg) -scale production, in particular for the utilization of expensive stable isotopes, are not well compiled in the literature. Therefore, in the interest of assisting future investigations into the molecular basis of antibiotic action and resistance, we provide detailed growth, labeling, and isolation protocols.

The Supplementary Information (SI) presented below contains the entire methodology and protocols discussed in the main text and we additionally include a compendium of additional experiments that may be useful to interested researchers in the SI section 6 (Appendix: Additional Information) for clarity. Contained within are other media formulations that did and did not work for the various fungal strains, <sup>15</sup>N-isotopic enrichment, and pictures of cultures that are characteristic of success or failure for production of antibiotics.

### 1.2 ***Chemicals***

<sup>13</sup>C and <sup>15</sup>N labeled compounds (see SI sections 6.1.4 and 6.1.5) were obtained from Cambridge Isotopes Laboratories, Spectra Stable Isotopes or Sigma-Aldrich, including: D-methionine ((1-<sup>13</sup>C, 99%) 96% chemical purity), L-methionine ((1-<sup>13</sup>C, 99%) 98% chemical purity), L-cysteine ((1-<sup>13</sup>C, 99%) 98% chemical purity), ethylamine hydrochloride (<sup>15</sup>N, 99%), ammonium sulfate (<sup>15</sup>N, 99%), and ammonium chloride (<sup>15</sup>N, 99%).

The following chemicals (vendors in parentheses) were used for solid and liquid media cultures: sucrose (Sigma), D-glucose (Sigma), D-(+)-lactose monohydrate (J.T. Baker), sodium chloride (Fisher), ammonium sulfate (Sigma), ammonium acetate (J.T. Baker), sodium sulfate (Sigma), glycerol (Fisher), peptone (Fisher), yeast extract (Fisher), citric acid (Sigma), agar (), corn steep solids (Sigma), potassium chloride (Sigma), potassium phosphate dibasic (Sigma), potassium phosphate monobasic (Sigma), L-asparagine (Sigma), DL-methionine (Sigma), L-cysteine (Alfa Aesar), starch from corn (Sigma; practical grade), soluble starch (Sigma), phenylacetic acid (Sigma), sodium nitrate (J.T. Baker), ethylammonium chloride (EMD Millipore), magnesium sulfate heptahydrate (Sigma), iron (II) sulfate heptahydrate (Sigma), zinc sulfate heptahydrate (J.T. Baker), manganese (II) sulfate monohydrate (J.T. Baker), cobalt (II)

sulfate (J.T. Baker), copper (II) sulfate pentahydrate (J.T. Baker), magnesium chloride hexahydrate (Fisher), sodium citrate dihydrate (Sigma), manganese (II) chloride tetrahydrate (EMD Millipore), zinc acetate dihydrate (J.T. Baker), iron (III) chloride hexahydrate (J.T. Baker), calcium chloride dihydrate (EMD Millipore), copper (II) chloride (Sigma), cobalt (II) nitrate hexahydrate (Sigma), ammonium molybdate tetrahydrate (Sigma), sodium tetraborate decahydrate (J.T. Baker), malt extract (BD Difco), calcium sulfate dihydrate (Sigma), copper (II) sulfate pentahydrate (J.T. Baker), ammonium iron (III) sulfate dodecahydrate (Sigma), calcium carbonate (J.T. Baker), ammonium iron (II) sulfate hexahydrate (Sigma), iron (II) chloride tetrahydrate (J.T. Baker), magnesium chloride hexahydrate (Fisher), zinc acetate dihydrate (J.T. Baker), copper (II) acetate monohydrate (J.T. Baker), penicillin G sodium salt (Sigma), cephalosporin C zinc salt (abc r GmbH), cefotaxime sodium salt (Cayman Chemicals), 7-aminocephalosporanic acid (Sigma).

For HPLC and LC-MS, HPLC grade acetonitrile (Fisher Chemical) and a 2 M triethylammonium acetate stock (Glen Research) was used. For the chemical conversion of 7-ACA to CTX (Scheme 1, red box), anhydrous dichloromethane (> 99.8 %) was obtained from Fisher Chemical, triethylamine (for synthesis) from Sigma Aldrich, and 2-mercaptobenzothiazolyl thioester of (Z)-2-[2-aminothiazol-4-yl]-2-methoxyimino acetic acid (MAEM) from Toronto Research Chemicals.

### 1.3 Fungal Strains

All organisms were acquired from the American Type Culture Collection (ATCC) and revived from either freeze-dried or frozen ampoules according to ATCC documentation. Penicillin was produced using *Penicillium rubens* (ATCC 28089; deposited as *Penicillium chrysogenum*) and is referred to as WIS 54-1255, a low-producing progenitor strain for industrial *Penicillium* sp.<sup>[2]</sup> Cephalosporin C was produced from an early improved strain of *Acremonium chrysogenum*, referred to as CW-19 (ATCC 36225). Materials sent from ATCC were revived on solid media indicated in their documentation (and see additional solid media recipes below) with notable morphology changes dependent on the media formulation resulting in either mycelium growth and/or sporulation after approximately 6-9 days. Note that cultures of ATCC 36225 were sent with an additional contaminant of some unknown organism that was found to outcompete CW-19 on all solid and liquid media used herein, leading to minimal or non-existent production of cephalosporin C as determined by HPLC analysis. However, CW-19 was occasionally found on plates as evidenced by slight yellow coloration of the agar.<sup>[3]</sup> CW-19 was isolated from the contaminant by serial dilution of collected spores (>10<sup>6</sup> -fold) and subsequent re-plating and dilution until single colonies could be isolated and separated. After this process, no further contamination of the solid media was observed and the contaminant strain was found not to produce cephalosporin C by HPLC analysis. Spores from individually isolated and propagated CW-19 colonies, which were used in this study to successfully produce cephalosporin C, were provided to ATCC. For further details see SI section 6.2.2.

### 1.4 General Information

All spore-containing materials were wrapped in medical tape (3M Micropore Surgical Tape 1530-3). Furthermore, all liquid culture flasks were sterilized prior to use with a cotton plug

(Fisher Scientific). Any material containing spores was handled with single-use serological pipets.

Glycerol stocks of spore solutions, filtered using 100  $\mu\text{m}$  cell strainers (Fisher), were produced using either a 0.9% (w/v) sodium chloride (saline) solution or 100 mM potassium phosphate (pH 7.4) buffer diluted 1:1 (v/v) with a 50% glycerol (v/v) aqueous solution, mixed in cryovials, and then immediately flash-frozen in liquid nitrogen and stored at  $-80^\circ\text{C}$ . Glycerol stocks were revived by re-plating of approx. 100  $\mu\text{L}$  of glycerol stock on solid agar plates.

### **1.5 Instrumentation and Analysis**

Mass spectrometry was performed in the Stanford University Mass Spectrometry facility of the Vincent Coates Foundation on a Waters Single Quadrupole LC-ESI/MS instrument. For direct injection experiments the analyte was dissolved in HPLC-grade acetonitrile at a concentration of 50  $\mu\text{M}$  and detected in ESI- mode at standard cone voltage. Alternatively, the analyte was dissolved in 2% acetonitrile:water and LC/MS was performed.

HPLC analysis and/or purification was performed using an Agilent 1260 Infinity system equipped with a 100  $\mu\text{L}$  or 2 mL injection loop and an analytical Alltech Absorbosphere C18 (5  $\mu\text{m}$ , 250 mm x 4.6 mm) or a preparative Agilent Prep-C18 column (10  $\mu\text{m}$ , 250 mm x 21.2 mm) using a detection wavelength of 220 or 250 nm for PenG and 250 nm for CPC, 7-ACA and CTX. All samples were filtered through a 10 kDa spin filter (Amicon Ultra – 0.5 mL) for 10 min at 14,000x g's and the flowthrough was diluted in a ratio of 1:9 with an aqueous 50 mM triethylammonium acetate (TEAA) solution and an addition of 5 % (v/v) acetonitrile (ACN). HPLC runs consisted of an initial phase of 5 min at 5 % ACN in 50 mM TEAA and a subsequent gradient of increasing ACN by 1% per min at flow rates of 1  $\text{mL min}^{-1}$  or 5  $\text{mL min}^{-1}$  on the analytical or preparative column, respectively. Assignment of elution peaks was performed using commercial standards (confirmed via doping of the pure chemical into media as a reference) and/or mass spectrometry analysis after isolation of peak fractions.

FTIR spectra were recorded on a Bruker Vertex 70 spectrometer with a liquid nitrogen-cooled mercury cadmium telluride (MCT) detector. A liquid cell was prepared using two  $\text{CaF}_2$  optical windows (19.05 mm diameter, 3 mm thickness, Lambda Research Optics, Inc.), separated by two semicircular Teflon spacers (25 and 50  $\mu\text{m}$  thickness). Reference spectra of 10 mM  $^{12}\text{C}$ - and  $^{13}\text{C}$ -PenG and CTX in  $\text{D}_2\text{O}$  buffer (50 mM  $\text{KPi}$ , 100 mM  $\text{NaCl}$ , pD 7.0) were acquired through averaging 256-512 scans from 4000-1000  $\text{cm}^{-1}$  with 1  $\text{cm}^{-1}$  resolution after 600 secs of dry air purging. Spectra of the PenG-TEM1 E166N complex was recorded at concentration of 2.7 mM PenG and 2.2 mM protein. Characteristic features of these  $\beta$ -lactam antibiotics appear in the mid-IR spectral range of 1800-1600  $\text{cm}^{-1}$ , and features below 1600  $\text{cm}^{-1}$  are not considered due to spectral overlap with vibrational modes from water, protein, salts, etc. All data processing was performed using OPUS software (Bruker). For further details about sample preparation see below (Section 5.5).

NMR spectra were obtained using a Varian Inova 500 MHz NMR spectrometer and referenced to 2,2-dimethyl-2-silapentane-5-sulfonate (see Section 5.6 for further details). A standard NMR tube was filled with a ca. 0.5 mM  $^{13}\text{C}_{\text{CO}}$ -PenG solution or a ca. 0.7 mM  $^{13}\text{C}_{\text{CO}}$ -PenG-TEM1 E166N mixture in 0.5 mL  $\text{D}_2\text{O}$  buffer.  $^{13}\text{C}_{\text{CO}}$ -PenG was recorded using 512 scans of a  $45^\circ$  pulse, 1.5 s of acquisition time, 1 s of delay time a sweep width of 33003 Hz; 0.5 Hz exponential apodization was used in the presented spectrum. For the  $^{13}\text{C}_{\text{CO}}$ -PenG-TEM1 E166N

complex 2292 scans were acquired with a delay time of 2 sec, and the displayed spectrum used an exponential apodization of 5 Hz, but conditions were otherwise identical. Note that this apodization does not lead to a broadening of the observed  $^{13}\text{C}_{\text{CO}}$ -PenG peak due to its width of 15 Hz in the protein. All spectral processing was performed using the MNova software suite. See section 5.6 for further details on the sample preparation.

## **2. $^{13}\text{C}_{\text{CO}}$ -Incorporation in Penicillin G with *Penicillium rubens* WIS 54-1255**

### **2.1 Solid Media**

In order to inoculate starter growths, WIS 54-1255 was grown on Power Medium<sup>[4]</sup> for 5-7 days until sporulation was observed as evidenced by a high density of blue-green spores (see example Figure S1). Power medium agar contains the following in g/L: 25 sucrose, 5 lactose monohydrate, 2.5 peptone, 0.5 corn steep solids, 52 potassium chloride, 1 sodium nitrate, 0.25 dibasic potassium phosphate, 0.03 monobasic potassium phosphate, 0.275 magnesium sulfate heptahydrate, 2 sodium chloride, 0.0005 copper (II) sulfate pentahydrate, 0.0015 iron (III) chloride hexahydrate, 20 agar. Higher densities of spores generally correlated with larger penicillin yields. Spores were harvested from agar plates by adding 10 mL of 0.9% (w/v) NaCl in deionized water to each plate. The mycelium and spores were scraped using a cell streaker and transferred via serological pipet through a 100  $\mu\text{m}$  cell strainer (Fisher). Each 25mL starter culture was inoculated with 2 mL of the saline spore solution flowthrough. See SI section 6.1.1 for additional solid media recipes that yielded production of penicillin G.



*Figure S1: (Left) Mycelium presenting after 3-4 days on Power Medium agar plate. (Right) Sporulating Power Medium agar plate after approximately 5-7 days of growth. Blue/green coloration is indicative of sporulation in WIS 54-1255. Mycelium is evidenced by a white coloration. WIS 54-1255 is very hydrophobic, and requires physical perturbation, generally with a sterile serological pipet or cell streaker to disperse spores into solution.*

### **2.2 Starter Media**

Starter cultures of 25 mL were made through dilution of 2 mL of Power Medium spore solution into 23 mL of filtered media (pH 5.7) containing in g/L: 40 glucose, 10 citric acid, 3 sodium acetate, 3 ethylammonium chloride, 5 ammonium sulfate, 1 monobasic potassium phosphate, 0.5 magnesium sulfate heptahydrate, and 10 mL/L of a 100x trace element solution (final concentrations in g/L are 0.05 iron (II) sulfate heptahydrate, 0.01 zinc sulfate

heptahydrate, 0.01 copper (II) sulfate pentahydrate, 0.01 manganese sulfate tetrahydrate, 0.005 cobalt (II) sulfate, and 0.001 sodium chloride) dissolved in deionized water. Starter cultures were shaken at 200 rpm in a rotary shaker at 25C for 24 hrs before transferring to Penicillin Production Media (PPM+) as discussed below in SI section 2.3. See the SI section 6.1.2 for additional starter media recipes that yielded Penicillin G.

### 2.3 Penicillin Production Media

Penicillin production was carried out in a modified media formulation derived from a combination of MDFP and PPM , referred to throughout the manuscript as PPM+. [5-6] As determined via HPLC, minimal (<0.01 mg/50mL) Penicillin G was produced in the absence of ethylammonium chloride in the production media. All PPM+ media formulations were sterile-filtered (0.22 µm) immediately before use. The final media, PPM+ (pH 6.3) contained in g/L: 75 lactose monohydrate, 5 glucose, 10 citric acid, 5 ammonium acetate, 4 sodium sulfate, 3 ethylammonium chloride, 2.12 dibasic potassium phosphate, 5.1 monobasic potassium phosphate, 2.5 phenylacetic acid, and 10 mL of 100x Trace Elements solution (pH 6.3) (100x solution contains in g/L: 5 magnesium chloride hexahydrate, 0.5 sodium citrate dihydrate, 0.3 manganese (II) chloride tetrahydrate 0.2 zinc acetate dihydrate, 0.2 iron (III) chloride hexahydrate, 0.075 calcium chloride dihydrate, 0.02 copper (II) chloride, 0.02 cobalt nitrate hexahydrate, 0.01 ammonium molybdate tetrahydrate, 0.01 sodium tetraborate decahydrate). [7]

*Table S1.  $\beta$ -lactam production media (PPM+(S) for PenG production in the presence of 1-<sup>13</sup>C-cysteine.*

PPM+(S) (pH 6.3)	
Chemical	g/L
Glucose	5
Lactose monohydrate	75
Citric Acid	10
NaCl	3.2
Ethylammonium HCl	3
NH <sub>4</sub> Acetate	5
K <sub>2</sub> HPO <sub>4</sub>	2.12
KH <sub>2</sub> PO <sub>4</sub>	5.1
Phenylacetic acid	2.5
Trace Elements A (pH 6.3) [a]	10mL
L-Cysteine	4

[a] See SI section 2.3 for chemical compositions of Trace Elements A.

Sulfur-depleted media for site-specific  $^{13}\text{C}$ -incorporation, referred to as PPM+(S) (pH 6.3) contained in g/L (Table S1): 75 lactose monohydrate, 5 glucose, 10 citric acid, 5 ammonium acetate, 4 L-cysteine (or isotopic equivalent), 3.2 sodium chloride, 3 ethylammonium chloride, 2.12 dibasic potassium phosphate, 5.1 monobasic potassium phosphate, 2.5 phenylacetic acid, and 10 mL of 100x Trace Elements A solution described above. The media formulation for  $^{15}\text{N}$ -incorporation and LC-MS analysis are presented in the SI section 6.1.4.

In order to inoculate PPM+ media, and all media formulations, 7 mL of starter media was transferred to a 15 mL tube and centrifuged at 4000x g's for 20 mins at 25C. Supernatant solution was decanted, and the cells were resuspended in the final media to be used with the sulfur-containing chemicals removed. After resuspension in the S-depleted PPM+ media, the tubes were spun again for 4000x g's for 20 mins at 25C. Supernatant was decanted and cells were transferred and washed with 50 mL of final PPM+ (or PPM+(S)) media into 250 mL Erlenmeyers flasks. Penicillin production flasks were shaken at 200 rpm in a rotary shaker at 25C for 7 days before extracting excreted Penicillin G. Flasks should increase in turbidity over time, with increasingly viscous media after 7 days.

## 2.4 Penicillin G Extraction & Purification

After 7 days of shaking, cells and media were passed through 100  $\mu\text{m}$  cell strainers, resulting in approximately 40 mL of liquid media. Filtered media was then spin-filtered in EMD Millipore Amicon 10 kDa MWCO filter units to remove any proteins or large cell debris that passes through the cell strainer.

Filtered media was then lyophilized resulting in approximately 2 – 3 g per 50 mL of PPM+(S) media. Ca. 300 mg of the dry mass was then diluted in 1.5 – 2 mL HPLC buffer (5 % acetonitrile in 50 mM aqueous triethylammonium acetate) for preparative HPLC isolation and purification of ca. 2 mg of PenG per run (Figure S2). The fractions were lyophilized for 2-3 days to remove trace amounts of triethylammonium acetate buffer before subsequent FTIR and MS analysis. IR spectroscopy:  $\nu(^{12}\text{C}=\text{O})/\nu(^{13}\text{C}=\text{O}) = 1762/1713\text{ cm}^{-1}$ . Mass spectrometry (ESI-)  $m/z$ : 333.92 [ $^{13}\text{C}_{\text{CO}}$ -PenG-H] $^-$ ; 333.02 [ $^{12}\text{C}_{\text{CO}}$ -PenG-H] $^-$ .

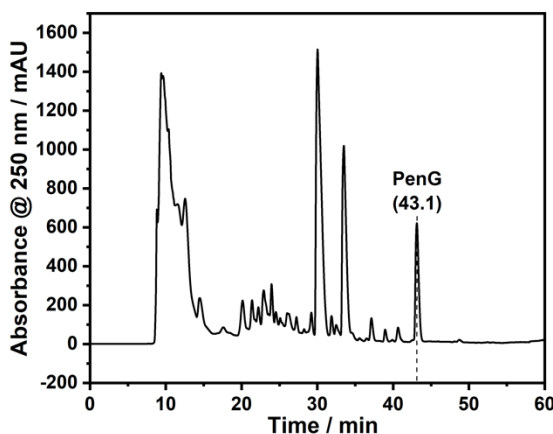


Figure S2. HPLC trace (preparative C18 column) of the purification and isolation of PenG (elution peak at 43.1 min) from the WIS54-1255 growth medium after 7 days.

## 2.5 PenG MS Fragmentation: Site-Specific Labeling



Analysis of the LC-MS fragmentation of the  $^{13}\text{C}_{\text{CO}}$ -PenG relative to the standard  $^{12}\text{C}$ -PenG provides further confirmation of the site-specificity of the  $^{13}\text{C}$ -incorporation at the  $\beta$ -lactam C=O. As shown in Figure 1 and Figure S3, the ESI- MS indicates that the molecular mass of 333.92 Da corresponding to  $[\text{}^{13}\text{C}_{\text{CO}}\text{-PenG} - \text{H}]^-$ . Similarly, the observed  $m/z$  at 289.93 Da corresponds to further fragmentation of the  $^{13}\text{C}_{\text{CO}}$ -PenG at the carboxylic acid ( $[\text{PenG} - \text{F}_1]^-$ ), in support of the  $^{13}\text{C}$ -incorporation at the  $\beta$ -lactam C=O, since the phenylacetic acid side-chain is added chemically to the media. Further fragmentation, with  $m/z$  at 191.9 Da, indicates that fragmentation along the penam-core leads to loss of the  $^{13}\text{C}$ -label, i.e.  $[\text{F}_2]^-$ . While these plausible assignments are not definitive, the obvious positions for  $^{13}\text{C}$ -incorporation (i.e. the carboxylic acid or  $\beta$ -lactam C=O), can be ruled out based on fragmentation, *in situ* chemical addition of phenylacetic acid, and further analysis below using IR and density functional theory (DFT) (section 5.1).

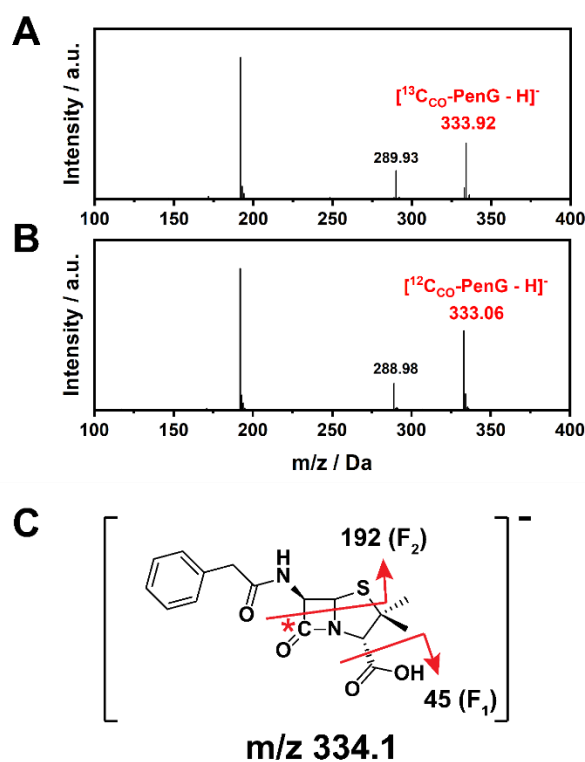


Figure S3. LC-MS spectrum of PenG. MS of (A)  $^{13}\text{C}_{\text{CO}}$ -PenG and (B)  $^{12}\text{C}_{\text{CO}}$ -PenG with isotope-incorporated masses indicated above. C: Fragmentation of PenG along the red arrows leads to indicated mass changes ( $\text{F}_1$  and  $\text{F}_2$ ; assuming  $^{12}\text{C}$  on fragments). The position of  $^{13}\text{C}$ -incorporation is indicated by the red asterisk.

### 3. $^{13}\text{C}_{\text{CO}}$ -Incorporation in Cephalosporin C with *Acremonium chrysogenum* CW-19

#### 3.1 Solid Media

In order to inoculate starter growths, CW-19 was grown on solid agar, referred to here as “SWD” for 7-10 days until sporulation was observed as evidenced by a high density of yellow colonies and surrounding agar (Figure S4).<sup>[8]</sup> SWD agar contains the following in g/L: 20

sucrose, 4 yeast extract, 4 peptone, 3 sodium nitrate, 0.5 dibasic potassium phosphate, 0.5 monobasic potassium phosphate, 0.5 potassium chloride, 0.5 magnesium sulfate heptahydrate, 0.01 iron (II) sulfate heptahydrate, 20 agar. Spores were harvested from agar plates by adding 10 mL of 0.1M potassium phosphate buffer (pH 7.4) in deionized water to each plate. The mycelium and spores were scraped using a sterilized spatula and transferred via serological pipet through a 100  $\mu$ m cell strainer. Each 25mL starter culture was inoculated with 2 mL of the spore solution flowthrough. Note that high-densities of spores from SWD plates can lead to aggregation of fungi in the starter media, which is prohibitive for transfer into production media. As needed, dilutions of 5-to-10-fold were enough to ensure sufficient dispersion after 48hrs of starter growth.



*Figure S4: (Left) bottom-view, (middle) front-view (without back-illumination), (right) front-view (with back-illumination).*

### **3.2 Starter Media**

Starter cultures of 25 mL in 250 mL Erlenmeyer flasks were made through dilution of 2 mL of SWD spore solution into 25 mL of autoclaved media (pH 7.0 before autoclaving) containing in g/L: 10.0 glucose, 15.0 soluble starch, 5.0 corn steep solids, 4.0 yeast extract, 1.0 dibasic potassium phosphate, 1.0 magnesium sulfate heptahydrate, 1.0 calcium carbonate dissolved in deionized water.<sup>[9]</sup> Starter cultures were shaken at 200 rpm in a rotary shaker at 25C for 48 hrs before transferring to cephalosporin C Defined Production Media (DFM) as discussed below in SI section 3.3.

### **3.3 Cephalosporin C Production Media**

Cephalosporin C production was carried out in a media formulation derived from DFM.<sup>[8]</sup> All DFM media formulations were sterile-filtered (0.22  $\mu$ m) immediately before use. The final media, DFM (pH 7.4) contained in g/L: 36.0 sucrose, 27.0 glucose, 12.0 L-Asparagine, 3.2 DL-Methionine, 0.16 ammonium iron(II) sulfate hexahydrate, and 140mL/L of Trace Elements B. Trace Elements B (pH 6.8) contains the following in g/L (salts dissolved in reverse-order): 115.5 dibasic potassium phosphate, 103.3 monobasic potassium phosphate, 5.55 sodium sulfate, 2.72 magnesium sulfate heptahydrate, 0.22 zinc sulfate heptahydrate, 0.22 manganese (II) sulfate monohydrate, 0.42 calcium chloride dihydrate, 0.055 copper (II) sulfate pentahydrate.

Table S2.  $\beta$ -lactam production media DFM(S) for CPC production in the presence of 1- $^{13}\text{C}$ -cysteine.

DFM(S) (pH 7.4)	
Chemical	g/L
Glucose	27
Sucrose	36
L-Asparagine	12
DL-Methionine	3.2
$\text{KH}_2\text{PO}_4^{[b]}$	16.2
$\text{K}_2\text{HPO}_4^{[b]}$	14.5
$\text{FeCl}_2 \times 4\text{H}_2\text{O}$	0.08
Trace Elements B (pH 6.8) <sup>[a]</sup>	140mL/L
L-Cysteine	2.6

<sup>[a]</sup> See SI section 3.3 for chemical compositions of Trace Elements B.

<sup>[b]</sup> Phosphate salts are part of the Trace Elements B solution; indicated concentrations (g/L) are those in the final DFM(S) solution.

Sulfur-depleted media for site-specific  $^{13}\text{C}$ -incorporation, referred to as DFM(S) (pH 7.4) contained in g/L (Table S2): 36.0 sucrose, 27.0 glucose, 12.0 L-asparagine, 2.6 L-cysteine (or isotopic equivalent), 0.08 iron (II) chloride tetrahydrate, and 140mL/L of Trace Elements B. Trace Elements B (pH 6.8) contains the following in g/L (salts dissolved in reverse-order): 115.5 dibasic potassium phosphate, 103.3 monobasic potassium phosphate, 4.57 sodium chloride, 2.24 magnesium chloride hexahydrate, 0.17 zinc acetate dihydrate, 0.26 manganese (II) chloride tetrahydrate, 0.044 copper (II) acetate monohydrate, 0.42 calcium chloride dihydrate.

In order to inoculate DFM media, 2 mL of starter media was transferred to a 15 mL tube, diluted 5-fold with the final media to be used with the sulfur-containing chemicals removed, and centrifuged at 4000xg's for 20 mins at 25C. The media solution was decanted, and the cells were resuspended in the sulfur-depleted final media again and centrifuged under identical conditions. After a final decanting, the cells were resuspended in the final sulfur-containing DFM media and transferred to an autoclaved 250 mL Erlenmeyer flask with a cotton plug. Production flasks were shaken at 200 rpm in a rotary shaker at 25C for 7-21 days before extracting excreted cephalosporin C as determined by HPLC analysis following daily sampling. The solutions inside the flasks should increase in turbidity and yellow coloration over time. Note that the replacement of sulfate with cysteine and methionine as the exclusive source of sulfur can lead to fungal morphology changes in solution, which has been reviewed extensively.<sup>[10-12]</sup> Noticeably, the heterogeneity of growths can be directly observed by the media morphology of cells, with slow production evidenced by swollen and spherical particles (Figure S5, right), whereas the fastest onset of antibiotic production is coincident with fragmentation of the mycelia

resulting in a cloudy media and gradually increasing yellow coloration (similar to the color of CW-19 on agar after ca. 7-10 days, Figure S5, left).<sup>[10]</sup> Furthermore, this heterogeneity led to a marked difference in CPC production as observed using HPLC (Figure S6). We speculate that slower fermentation results in increased protein catabolism and/or amino acid biosynthesis of serine (converted to cysteine via cystathionine), methionine (S-atom exchanged onto cysteine via homocysteine), and cysteine, leading to isotopic dilution.



Figure S5. CW-19 growth heterogeneity after 6 days of production media. (Left) Idealized appearance of DFM(S) media after approximately 3-7 days with turbid yellow media. (Right) Evidence of slow CW-19 growth in DFM(S) with characteristic spherical particles and minimally turbid media. Both flasks shown were produced from plates and starter media propagated identically and at the same time of onset.

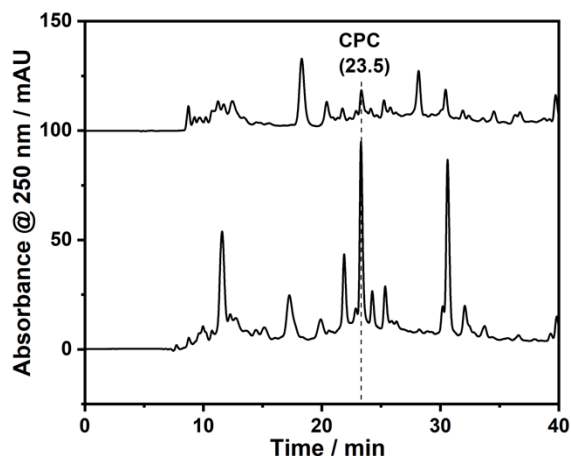


Figure S6. HPLC traces (preparative C18 column) displaying the CW-19 growth heterogeneity after 12 days of production media. HPLC traces were recorded at identical conditions and show the range of CPC content (elution peak at 23.5 min) between two independent growths yielding in an estimated final and isolatable CPC amount of 0.01 – 0.06 mg/mL.

### 3.4 Cephalosporin C Extraction & Purification

After maximal CPC production (~15 days), CPC-containing media was removed by centrifugation at 4000x g's for 20 min at 25C and subsequent washing with water. The media

was then filtered sequentially using 5, 0.45, and then 0.22  $\mu\text{m}$  filters, after which the final filtered media was lyophilized to enable efficient loading for HPLC purification. Note that DFM(S) that only contained L-cysteine was observed to be more difficult to filter and load onto the HPLC column.

Lyophilized media resulted in ca. 3 g of dry mass. The dry mass in ca. 200 mg aliquots was then diluted in 1.5 – 2 mL HPLC buffer (5 % acetonitrile in 50 mM aqueous triethylammonium acetate) for preparative HPLC isolation and purification of ca. 50 - 300  $\mu\text{g}$  of CPC per run (depending on the total yield in the entire dry mass). The fractions were lyophilized for 2-3 days to remove trace amounts of triethylammonium acetate buffer before subsequent FTIR and MS analysis. Mass spectrometry (ESI-)  $m/z$ : 415.12 [ $^{13}\text{C}_{\text{CO}}$ -CPC-H] $^-$ ; 414.03 [ $^{12}\text{C}_{\text{CO}}$ -CPC-H] $^-$ . Mass spectrometry (ESI+)  $m/z$ : 417.12 [ $^{13}\text{C}_{\text{CO}}$ -CPC+H] $^+$ ; 416.16 [ $^{12}\text{C}_{\text{CO}}$ -CPC+H] $^+$ .

### **3.5 Conversion of CPC to 7-ACA, and 7-ACA to CTX**

The combined CPC fractions (containing ~ 550  $\mu\text{g}$  CPC) were dissolved in 5 mL of 50 mM phosphate buffer (pH 8.0) and treated with 2  $\mu\text{M}$  CPCA at 4C overnight in order to produce 7-ACA (see section 4.4 below). 7-ACA was purified using preparative HPLC and yielded 360  $\mu\text{g}$ . Note that addition of CPCA to filtered media was not observed to convert CPC to 7-ACA, potentially due to inhibition or the higher metabolite/salt concentrations, which may lead to dissociation of the heterodimer (SI section 4.3 and 4.4).

7-ACA was directly subjected to the chemical step in order to obtain CTX.<sup>[13]</sup> Here, 360  $\mu\text{g}$  of 7-ACA was dissolved in 1 mL dichloromethane. 0.41  $\mu\text{L}$  triethylamine (2.2 eq.) and 0.5  $\mu\text{g}$  MAEM (1.1 eq) were added under ice cooling. The reaction was stirred at RT for 3 h after which the solvent was removed under reduced pressure. The residue was dissolved in 1.5 mL of 5 % acetonitrile in 50 mM aqueous triethylammonium acetate and purified on a preparative C18 column using HPLC to obtain 390  $\mu\text{g}$  CTX (65 %). IR spectroscopy:  $\nu(^{12}\text{C}=\text{O})/\nu(^{13}\text{C}=\text{O}) = 1764/1716\text{ cm}^{-1}$ . Mass spectrometry (ESI-): 455.24 [ $^{13}\text{C}_{\text{CO}}$ -CTX-H] $^-$ ; 454.17 [ $^{12}\text{C}_{\text{CO}}$ -CTX-H] $^-$ . Mass spectrometry (ESI+)  $m/z$ : 457.21 [ $^{13}\text{C}_{\text{CO}}$ -CTX+H] $^+$ ; 456.12 [ $^{12}\text{C}_{\text{CO}}$ -CTX+H] $^+$ .

### **3.6 CPC and CTX MS Fragmentation: Site-Specific Labeling**

Further confirmation for the site-specific  $^{13}\text{C}$ -incorporation at the  $\beta$ -lactam C=O of CPC and CTX can be observed based on the LC/MS ESI+ and ESI- spectra.

In the case of CPC in ESI+ (Figure S7 A,B,E), molecular masses with an approximately 1:1 ratio of  $^{12}\text{C}$ - and  $^{13}\text{C}$ -labeling, i.e. +1 Da, are observed at 416.25 and 356.22 Da, corresponding to [CPC + H] $^+$  and [CPC – F<sub>4</sub>] $^+$  and/or [CPC – F<sub>2</sub>] $^+$ . Likewise, ESI- (Figure S7 C,D,E) indicates labeling at 414.03, 370.07, and 354.03, likely corresponding to [CPC – H] $^-$ , [CPC – H – (F<sub>1</sub> or F<sub>2</sub>)] $^-$ , and [CPC – F<sub>2</sub> – F<sub>3</sub>] $^-$ , respectively.

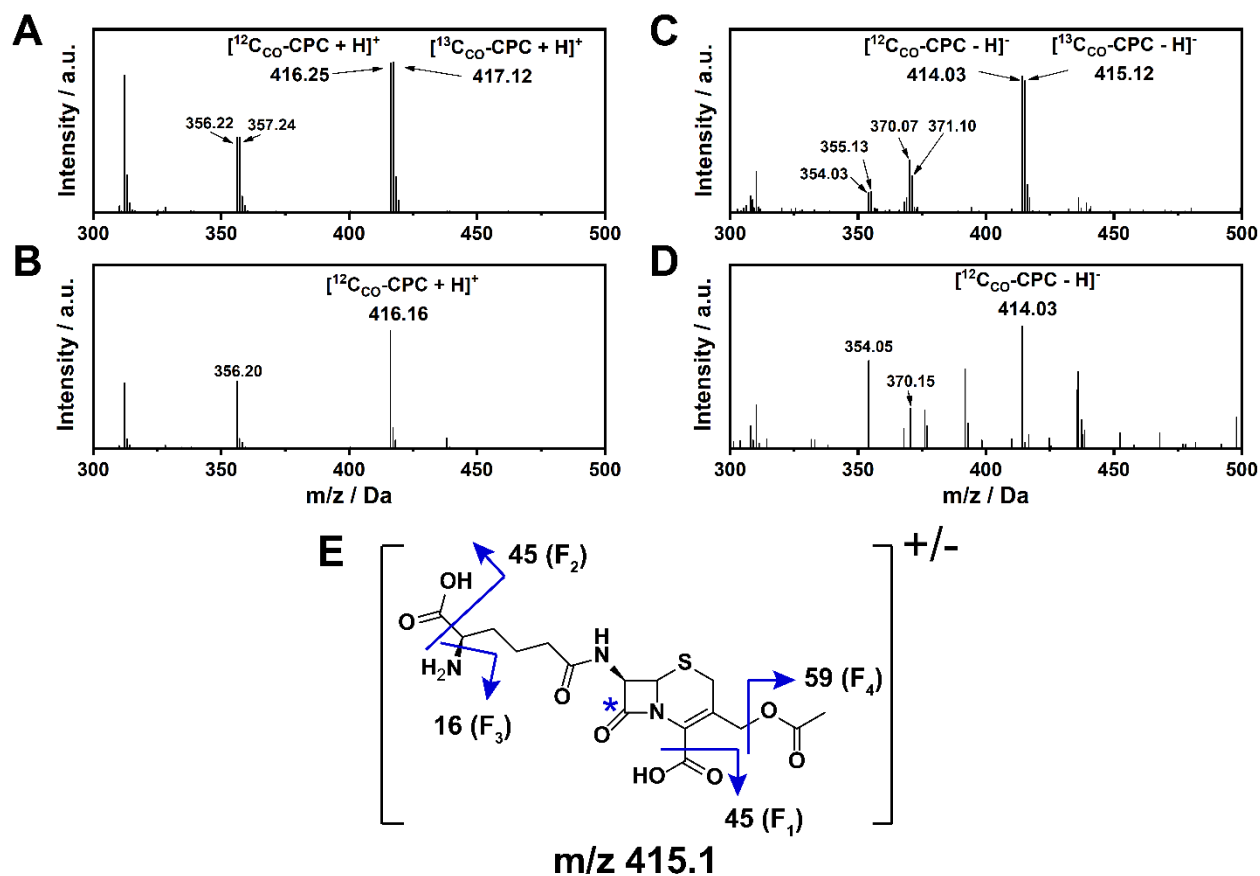


**Figure S7.** LC-MS spectra of CPC. Corresponding MS of  $^{13}\text{C}_{60}$ - and  $^{12}\text{C}_{60}$ -CPC in (A,B) ESI+ and (C,D) ESI- modes, respectively. Fragmentation masses are indicated above peaks where isotope is enriched at an ca. 1:1 ratio. E: Fragmentation of CPC along the blue arrows gives rise to the corresponding masses observed in panels A-D. The position of the  $^{13}\text{C}$  is denoted with an asterisk.

Analogous to the analysis with CPC, CTX exhibits a similar MS fragmentation pattern. In ESI+ (Figure S8 A, B, E), masses with an approximate 1:1 ratio of  $^{12}\text{C}$ - and  $^{13}\text{C}$ -labeling, are observed at 456.23, and 396.16, which likely correspond to  $[\text{CTX} + \text{H}]^+$ , and  $[\text{CTX} - \text{F}_1]^+$ , respectively. Dominant fragments that are absent of a corresponding  $^{13}\text{C}$ -label are observed at 368.2 and 324.2 Da, which may be due to fragments  $[\text{CTX} - \text{F}_1 - \text{F}_3]^+$  and  $[\text{CTX} + \text{H} - \text{F}_1 - \text{F}_2 - \text{F}_3]^+$ , respectively. In ESI- (Figure S8, C,D,E), labeled fragments are observed at 454.17, and 350.13 Da, indicative of fragments,  $[\text{CTX} - \text{H}]^-$ , and  $[\text{CTX} - \text{H} - \text{F}_1 - \text{F}_2]^-$ , respectively.

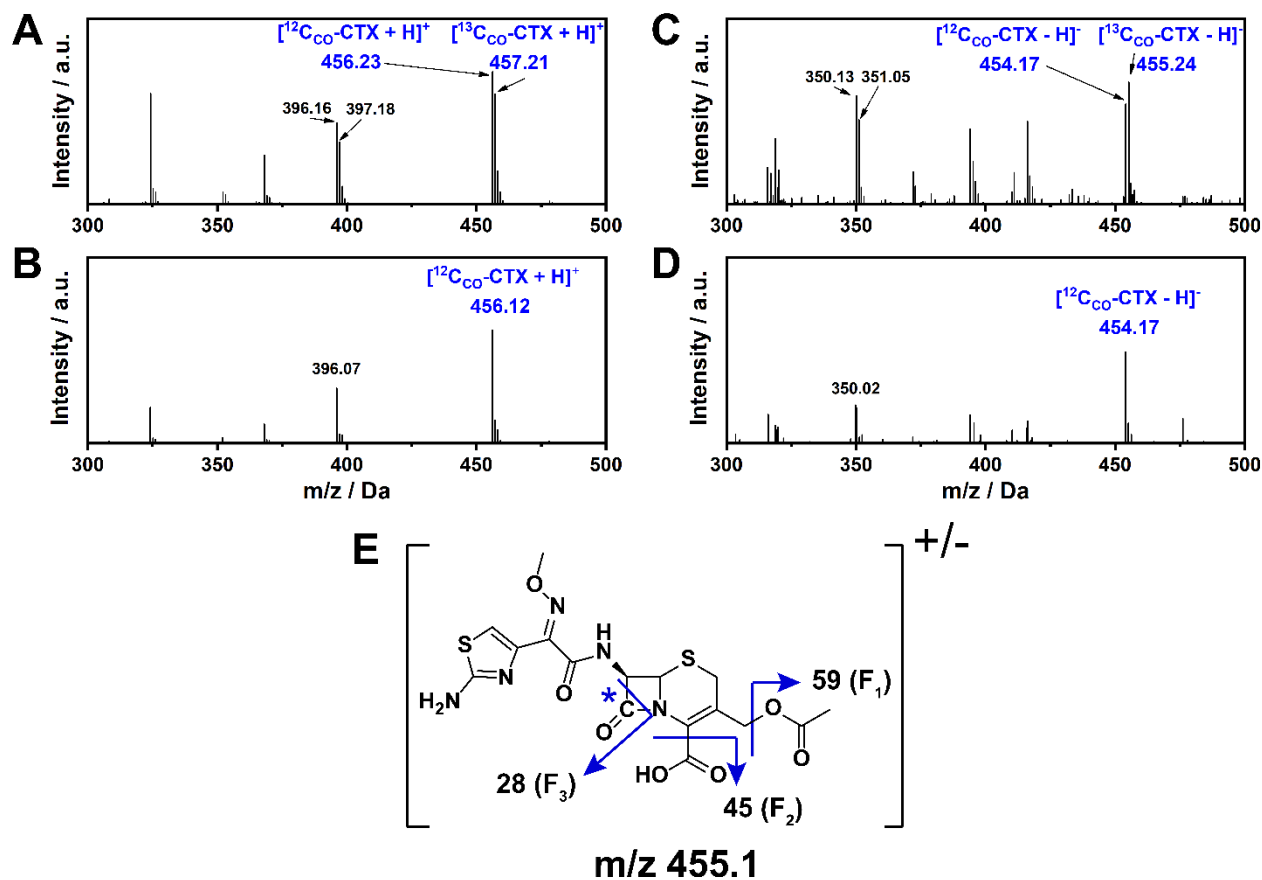


Figure S8. LC-MS spectra of CTX. Corresponding MS of  $^{13}\text{C}_{\text{CO}}\text{-}$  and  $^{12}\text{C}_{\text{CO}}\text{-CTX}$  in (A,B) ESI+ and (C,D) ESI- modes, respectively. Fragmentation masses are indicated above peaks where isotope is enriched at an ca. 1:1 ratio. E: Fragmentation of CTX along the blue arrows gives rise to the corresponding masses observed in panels A-D. The position of the  $^{13}\text{C}$  is denoted with an asterisk.

Based on the above identification and possible fragmentation patterns there is further support for the  $^{13}\text{C}$ -incorporation at the  $\beta$ -lactam  $\text{C}=\text{O}$ . Fragmentation indicates that the obvious other  $\text{C}=\text{O}$  groups (acetic acid side-chain and carboxylic acid) do not have  $^{13}\text{C}$  incorporated, and the CTX side-chain is added chemically *in vitro* after CPC synthesis, so it cannot be labeled. Therefore, in conjunction with the FTIR (Figure 2A,B), NMR (Figure 2C), and DFT (SI section 5.1) results, these all point to an unambiguous site-specific incorporation of the  $^{13}\text{C}_{\text{CO}}$ , attributable to this biosynthetic approach to isotope labeling.

## 4. Cephalosporin C Acylase

### 4.1 Plasmid construction of Cephalosporin C Acylase

The gene for CPCA was that from *Pseudomonas* sp. (Genbank Accession #: AAA25690) with the additional mutations, V122A, G140S, F297N, I314T, I415V, S710C, found

by Ma *et al.*<sup>[14-15]</sup> The gene was synthesized and purchased from GenScript and placed in the pET15b-plasmid vector between the restriction sites **NdeI** and **BamHI**, yielding a N-terminal His-tag and Thrombin cleavage site preceding the CPCA gene. For specific DNA and amino acid sequences (SI section 4.2) see below.

**CATATG**ACCATGGCGGCGAAAACCGATCGTGAGGCGCTGCAAGCGGCGCTGCCGCCGCT  
GAGCGGTAGCCTGAGCATTCCGGGTCTGAGCGCGCCGGTGCGTGTTACGCGTGACGGCT  
GGGGTATCCCGCACATTAAAGCGAGCGGTGAAGCGGATGCGTATCGTGCGCTGGGTTTTG  
TGCATGCGCAGGATCGTCTGTTTCAAATGGAGCTGACCCGTCGTAAAGCGCTGGGTCGTG  
CGGCGGAATGGCTGGGTGCGGAGGCGGCGGAAGCGGATATCCTGGTTCGTCTGTCTGGGT  
ATGGAAGAGTTTTGCCGTCTGACTTTGAGGCGCTGGGTGCGGAAGCGAAAGATATGCTG  
CGTGCGTACGCGGCGGGTGTTAACGCGTTTCTGGCGAGCGGTGCGCCGCTGCCGATTGA  
GTATAGCCTGCTGGGTGCGGAGCCGGAACCGTGGAACCGTGGCACAGCATTGCCGTGA  
TGCGTCTGTCTGGGTCTGCTGATGGGCAGCGTTTGGTTCAAGCTGTGGCGTATGCTGGCGC  
TGCCGGTGTTGGTGCGGCGAACGCGCTGAACTGCGTTACGACGATGGTGGCCAGGAC  
CTGCTGTGCATCCCGCCGGGCGTGAGGCGGAACGTCTGGAGGCGGACCTGGCGGCGC  
TGCGTCCGGCGGTTGATGCGCTGCTGAAGGCGATGGGTGGCGACGCGAGCGATGCGGC  
GGGTGGCGGTAGCAACAACCTGGGCGGTGGCGCCGGGTCGTACCGCGACCGGCCGTCGG  
ATCCTGGCGGGTGACCCGCACCGTGTTTTCGAAATTCCGGGCATGTATGCGCAGCACAC  
CTGGCGTGCGACCGTTTCGATATGATCGGTCTGACCGTGCCGGGTGTTCCGGGCTTTCCG  
CACAACGCGCACAACGGCAAAGTGCGTACTGCGTTACCCACGCGTTCATGGACACCCAC  
GATCTGTATCTGGAGCAATTTGCGGAAGACGGCCGTACCGCGCGTTTCGGTAACGAGTTT  
GAACCGGTGGCGTGCGGTCTGATCGTATTGCGGTTTCGTGGCGGTGCGGACCGTGAGTT  
TGATATCGTGGAACCCGTCACGGTCCGGTTATTGCGGGCGACCCGCTGGAGGGTGCGG  
CGCTGACCCTGCGTAGCGTGCA GTTCGCGGAACCGACCTGAGCTTTGATTGCCTGACCC  
GTATGCCGGGTGCGAGCACCGTGCGGCAACTGTATGATGCGACCCGTGGCTGGGGTCTG  
GTTGACCACAACCTGGTGGCGGGCGATGTTGCGGGTAGCATTGGTCACCTGGTGCGTGC  
GCGTGTTCCGAGCCGTCCGCGTGAGAACGGTTGGCTGCCGGTTCCGGGTTGGAGCGGTG  
AACACGAATGGCGTGCGTGATTCCGCACGAAGCGATGCCGCGTGTGATTGACCCGCCG  
GGCGGTCTGATTGTTACCGCGAACAACCGTGTGGTTGCGGACGATACCCGGACTACCTG  
TGCACCGATTGCCACCCGCCGTATCGTGCGGAGCGTATCATGGAACGTCTGGTGGCGAG  
CCCGGCGTTTGCGGTTGATGATGCGGCGGGCGATTCACGCGGATACCCTGAGCCCGCACG  
TTGGTCTGCTGCGTGCGGTCTGGAAGCGCTGGGTATCCAGGGCAGCCTGCCGGCGGAG  
GAACTGCGTCAAACCCTGATTGCGTGCGGATGGTCGTATGGATGCGGGTAGCCAGGCGGC  
GAGCGCGTACAACGCGTTCCGTCTGCGCTGACCCGTCTGGTTACCGCGCGTAGCGGTC  
TGGAACAAGCGATTGCGCACCCGTTTGCGGCGGTGCCGCCGGGCGTTAGCCCGCAGGGT  
CAAGTGTGGTGGGCGGTTCCGACCCTGCTGCGTAACGACGATGCGGGTATGCTGAAAGG  
TTGGAGCTGGGATGAAGCGCTGAGCGAAGCGCTGAGCGTGCGGACCCAAAACCTGACCG  
GTCGTGGTTGGGGCGAGGAACATCGTCCGCGTTTCACCCACCCGCTGAGCGCGCAATTC  
CGGCGTGGGCGGCGCTGCTGAACCCGGTTAGCCGTCCGATTGGCGGTGACGGTGATACC  
GTGCTGGCGAACGGCCTGGTTCCGAGCGCGGGTCCGGAGGCGACCTACGGCGCGCTGT  
GCCGTTATGTGTTGACGTTGGTAACCTGGGATAACAGCCGTTGGGTGGTTTTTCATGGTGC  
GAGCGGTCACCCGGCGAGCCCGCACTATGCGGACCAGAACGCGCCGTGGAGCGATTGC



GCGATGGTGCCGATGCTGTATAGCTGGGACCGTATTGCGGCGGAGGCGGTGACCAGCCA  
AGAACTGGTTCGGCGTAA**GGATCC**

#### 4.2 Protein Sequence Produced from pET15b-CPCA Plasmid

(Key: **Orange** = His-tag; **Green** = Thrombin Cleavage Site; **Blue** = Cleavage Site of G238/S239; **Red** = Start of Alpha-subunit; **Yellow** = Additional Mutations)

MGSS**HHHHHH**SSG**LVPRGS****HM**TMAAKTDREALQAALPPLSGSL SIPGLSAPVRVQRD GWGIP  
HIKASGEADAYRALGFVHAQDRLFQMELTRRKALGRAAEWLGAEEAEADILVRRLGMEKVCRR  
DFEALGAEAKDMLRAY**A**AGVNAFLASGAPLPIEY**S**LLGAEPWPWPWHIAVMRRLLGMLGMSV  
WFKLWRMLALPVVGAANALKLRYDDGGQDLLCIPPGVEAERLEADLAALRP AVDALLKAMGG  
DASDAAGG**GS**NNWAVAPGRTATGRPILAGDPHRVFEIPGMYAQHHLACDRFDMIGLTVPGVP  
GFP**N**AHNGKVAYCVTHAFMD**T**HDLYLEQFAEDGRTARFGNEFEPVAWRRDR IAVRGGADR  
EFDIVETR HGPVIAGDPLEGAALTLRSVQFAETDLSFDCLTRMPGASTVAQLYDATRGWGL**V**D  
HNLVAGDVAGSIGHLVRARVPSRPRENGWLVPVGWSGEHEWRGWIPHEAMPRVIDPPGGLIV  
TANNRVVADDHPDYLCTDCHPPYRAERIMERLVASPAFAVDDAAAIHADTLSPHVGLLRARLEA  
LGIQGS LPAEELRQTLIAWDGRMDAGSQAASAYNAFRRALTRLVTARSGLEQAI AHPFAAVPP  
GVSPQGGQVWWAVPTLLRNDDAGMLKGWSWDEALSEALSVATQNL TGRGWGEEHRPRFTHP  
LSAQFPAWAALLNPVSRPIGGDGD TVLANGLVPSAGPEATY**GALC**RYVFDVGNWDNSRWVVF  
HGASGHPASPHYADQNAPWSDCAMVPM LYSWDRIA AEAVTSQELVPA

#### 4.3 Protein expression and purification of CPCA

The pET15b-CPCA vector was transformed into BL21(DE3) *E. coli* cells using selection with 100 µg/mL ampicillin on Luria Broth (Fisher) agar plates. A single-colony of transformed cells was grown into 5 mL overnight cultures using Luria Broth with 100 µg/mL Ampicillin at 37°C. Overnight cultures were then inoculated into 1 L of Terrific Broth (Fisher) media with 100 µg/mL ampicillin shaking at 200 rpm and 37°C until they reached an OD<sub>600</sub> ~ 0.6 at which point they were induced with isopropyl β-D-1-thiogalactopyranoside (IPTG; Santa Cruz Biotechnologies) to a final concentration of 1 mM, and grown overnight at 23°C. Cells were harvested by centrifugation at 6000x g's for 30 min and resuspended in lysis buffer (50mM potassium phosphate, 20mM imidazole, 500mM sodium chloride, 10% (v/v) glycerol, pH 7.4). Cells were lysed by homogenization, and the lysate centrifuged twice for 90 mins each at 15,000x g's before sterile filtering the supernatant. The crude protein was then purified using a Ni-NTA (Qiagen) affinity resin column, washing with 50mM potassium phosphate (pH 7.4), 50mM imidazole, 500mM sodium chloride and eluted using 50mM potassium phosphate (pH 7.4), 200mM imidazole, 500mM sodium chloride. Further purification was performed using anion exchange chromatography on an FPLC (GE Healthcare, Äkta Purifier) with a 5mL HiTrap-Q HP (GE Healthcare) column and eluted using a 0-50% gradient of Buffer A (25mM Tris (pH 8.4) 25mM sodium chloride) to Buffer B (25mM Tris (pH 8.4) 1M sodium chloride) over 20 column volumes. CPCA was found to elute at two ionic strengths, 250 mM (fractions collected between 210-270 mM) and 320 mM (fractions collected between 295-340 mM), both fractions were collected and analyzed by LC-MS and functional kinetics as determined via conversion of CPC to 7-ACA. Chromatograms and MS analysis indicates that both fractions contain approx. a 1:1 ratio of the α- and β-subunits of CPCA (α-subunit ~ 27577 Da (expected 27568 Da for G2-

G238);  $\beta$ -subunit ~ 58153 Da (expected 58134 Da for S239-A794)), which are formed via autocatalytic cleavage between residues G238 and S239.<sup>[16]</sup> Based on maximum entropy integration (Waters MassLynx) of the LC-MS data, the ratio of the subunits was found to differ with the first fraction having ( $\alpha/\beta$ )>1 relative to <1 for the second fraction. However, the first fraction (eluting at 250 mM sodium chloride) was found to be more active and used exclusively for chemical conversion of CPC to 7-ACA, as discussed in SI sections 3.5 and 4.4. CPCA was exchanged into 50mM potassium phosphate (pH 8.0) with 10% (v/v) glycerol as a cryoprotectant for long-term storage at -80C.

#### 4.4 Reaction monitoring of CPCA activity with UV-vis and HPLC

Reaction progress of CPC to 7-ACA was monitored via UV-vis at either 279 or 254 nm (Figure S9A) and stoichiometric conversion was confirmed using HPLC of fractions taken before CPCA addition and after the UV-vis trace plateaued (Figure S9B). Note that with the above storage buffer, there was no observed loss of activity with multiple freezing and thawing. However, when stored in higher salt buffers ( $\geq 100$ mM), activity was found to decrease as a function of time (and with subsequent freezing and thawing), which may be due to dissociation of the heterodimer, although not extensively characterized herein.

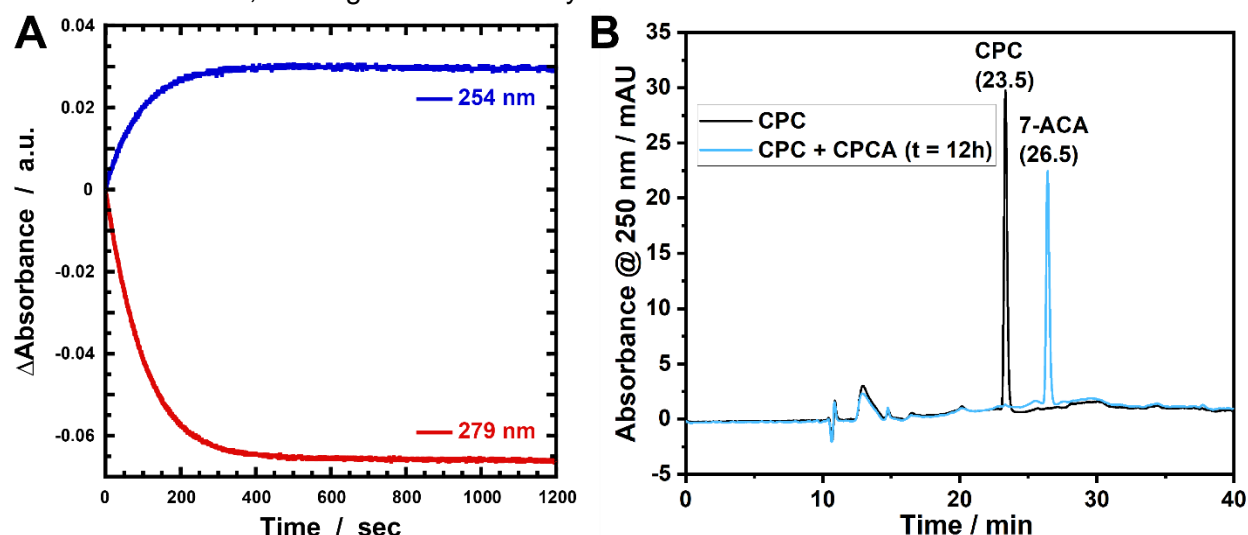


Figure S9. Stoichiometric conversion of commercial CPC to 7-ACA by CPCA. A: UV-vis trace of conversion of ca. 150  $\mu$ M CPC to 7-ACA in the presence of 2  $\mu$ M CPCA in 50mM phosphate buffer (pH 8.0), shown in terms of change in absorbance (absorbance at  $t = 0$  was taken as a reference). Changes in absorbance were monitored at either 254 (blue) or 279 (red) nm. B: HPLC (preparative C18 column) traces of CPC before addition of CPCA (black), and after 12 h of treatment with CPCA (light blue) under similar condition as used for the media-extracted CPC. The traces show full conversion from CPC to 7-ACA.

## 5. TEM-1 (E166N) $\beta$ -Lactamase

### 5.1 Assignment of $^{13}\text{C}=\text{O}$ mode of $\beta$ -lactam using DFT

In order to confirm the assignment and frequency shift due to isotopic labeling, density functional theory (DFT) was performed using Gaussian 09<sup>[17]</sup> (Rev. E-01; run on the Stanford Research Computing Center Farmshare2) employing the b3lyp functional and the 6-311++g(d,p) basis set. The options opt=tight and int=ultrafine were used during the optimization; int=ultrafine and freq for the normal mode analysis. Calculations were furthermore performed using a polarizable continuum model (scrf = ( solvent = water)). For the isotopically labeled compounds the  $\beta$ -lactam carbonyl carbon was specified to be  $^{13}\text{C}$ -labeled using "iso=13", i.e.  $^{13}\text{C}_{\text{CO}}$ . Simulated IR spectra are displayed using Gaussian-shaped peaks with an HWHM of 16  $\text{cm}^{-1}$ .

Figure S10 demonstrates the predicted isotope effect in the simulated IR spectra upon site-specifically  $^{13}\text{C}$ -labeling of PenG (A) and CTX (B, C) at the  $\beta$ -lactam carbonyl (also see Table S3 for additional mode assignments). The  $\beta$ -lactam C=O stretch of PenG is selectively shifted by ca. 46  $\text{cm}^{-1}$  while the remaining modes in the shown spectral window remain unchanged (dashed lines). Performing a difference of  $^{12}\text{C}_{\text{CO}}$ -PenG and  $^{13}\text{C}_{\text{CO}}$ -PenG results in 1<sup>st</sup> derivative lineshape reflecting this isotope shift due to the broad linewidths in aqueous buffer. For CTX (B) the same effect is observed. In the absolute spectra (dashed lines) the  $\beta$ -lactam C=O stretch is shifted by 46  $\text{cm}^{-1}$  leading to an overlap with the ester C=O stretch. As with PenG, the difference spectrum  $^{12}\text{C}_{\text{CO}} - ^{13}\text{C}_{\text{CO}}$  of CTX reveals the specific frequency shift of the labeled  $\beta$ -lactam carbonyl. For the sake of clearer comparison with experimental data in Figure 2B (main text), Figure S10C shows a comparison of  $^{12}\text{C}_{\text{CO}}$ -CTX and a 1:1 mixture of  $^{12}\text{C}_{\text{CO}}$ -CTX and  $^{13}\text{C}_{\text{CO}}$ -CTX (blue dashed line), where absolute spectra do not show a complete isotope shift, but the difference spectra provide a similar unambiguous isotope shift as in B with half the intensity.

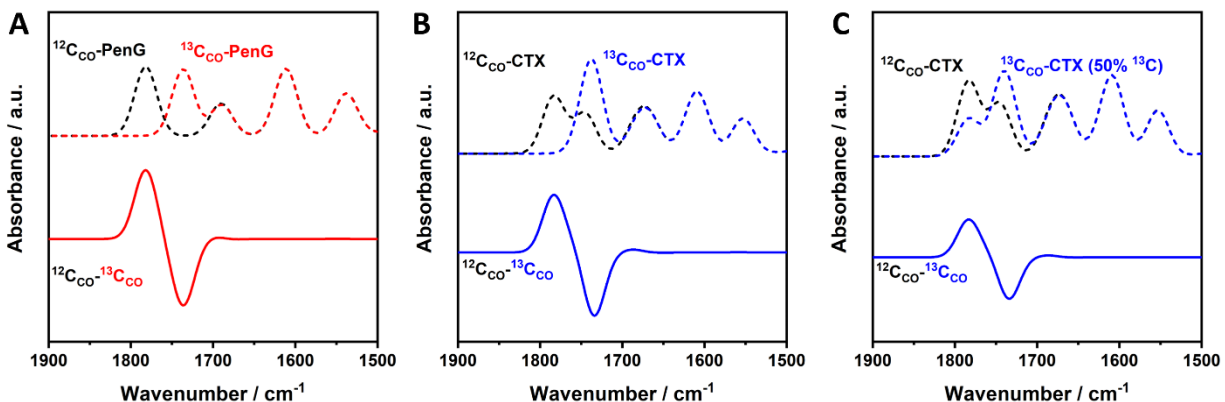


Figure S10. Simulated DFT-IR spectra of PenG (A) and CTX (B,C) displaying the isotope shift effect on the  $\beta$ -lactam C=O stretch due to site-specific  $^{13}\text{C}$ -labeling. The absolute spectra of are shown as dashed lines, while  $^{12}\text{C} - ^{13}\text{C}$  difference spectra are represented using solid lines. C: Representative absolute and difference spectra assuming a 1:1 mixture of  $^{12}\text{C}$ -CTX and  $^{13}\text{C}$ -CTX spectra for comparison with 100%  $^{13}\text{C}_{\text{CO}}$  incorporation as depicted in (B). This presents a direct comparison to the experimental IR difference spectra (Figure 2 in the main text) where a 50%  $^{13}\text{C}_{\text{CO}}$  incorporation was observed.

Table S3: Assignment of normal modes in the spectral region of 1800 – 1500  $\text{cm}^{-1}$  based on DFT calculations presented in Figure S10. Sidechain refers to either the phenylacetyl or (Z)-2-[2-aminothiazol-4-yl]-2-methoxyimino acetyl (AEM) side-chain.

PenG mode assignment	Freq. ( $^{12}\text{C}$ ) / $\text{cm}^{-1}$	Freq. ( $^{13}\text{C}$ ) / $\text{cm}^{-1}$	CTX mode assignment	Freq. ( $^{12}\text{C}$ ) / $\text{cm}^{-1}$	Freq. ( $^{13}\text{C}$ ) / $\text{cm}^{-1}$
$\nu(\text{C=O})_{\beta\text{-lactam}}$	1781.91	1736.37	$\nu(\text{C=O})_{\beta\text{-lactam}}$	1783.32	1736.74
amide I <sub>sidechain</sub>	1690.34	1689.68	$\nu(\text{C=O})_{\text{ester}}$	1745.55	1746.61
$\nu(\text{C=C})_{\text{aromatic}}$	1637.16	1637.16	amide I <sub>sidechain</sub>	1682.89	1682.19
$\nu(\text{C=C})_{\text{aromatic}}$	1619.69	1619.69	$\delta(\text{NH}_2)_{\text{sidechain}}$	1665.85	1665.85
$\nu(\text{COO}^-)_{\text{as}}$	1611.24	1611.24	$\nu(\text{C=C})$	1659.61	1659.83
amide II <sub>sidechain</sub>	1538.52	1538.49	$\nu(\text{C=C})_{\text{sidechain}}$	1628.51	1628.90
			$\nu(\text{COO}^-)_{\text{as}}$	1610.34	1610.34
			$\nu(\text{C=N})_{\text{sidechain}}$	1603.49	1603.49
			$\nu(\text{C=N})_{\text{sidechain}}$	1597.80	1597.80
			amide II <sub>sidechain</sub>	1553.20	1553.17

## 5.2 Nucleotide Sequence of TEM-1 E166N $\beta$ -Lactamase

The pBAD plasmid containing TEM-1 (pBAD-TEM-1)  $\beta$ -lactamase was kindly given to us by Patrice Soumilion at the Université catholique de Louvain. Using commercial QuickChange Lightning (Agilent) kits and protocols, standard PCR site-directed mutagenesis was performed the plasmid and transformed into DH10B *E. coli* cells with 15  $\mu\text{g}/\text{mL}$  tetracycline HCl selection on agar plates in order to introduce the E166N mutation and a Thrombin cleavage site, yielding the following His-tagged nucleotide sequence with protein sequence annotation below in section 5.2. The sequence-confirmed plasmid was transformed into One Shot TOP10 Chemically Competent *E. coli* cells (Thermo-Fisher) in the presence of Tetracycline HCl for protein expression and purification (see below Sections 5.2 and 5.3).

(Key: Green = His-tag; Red = Thrombin cleavage site; Pink = E166N mutation)

ATGGG TAGTCAACATTTCCGTGTCGCCCTTATTCCTTTTTTGCGGCATTTTGCCTTCCTGT  
TTTTGCTCACCCAGAAACGCTGGTGAAAGTAAAAGATGCTGAAGATCAGTTGGGTGCACGA  
GTGGGTTACATCGAACTGGATCTCAACAGCGGTAAGATCCTTGAGAGTTTTCGCCCCGAAG  
AACGTTTTTCCAATGATGAGCACTTTTAAAGTTCTGCTATGTGGCGCGGTATTATCCCGTGTT  
GACGCCGGGCAAGAGCAACTCGGTCGCCGCATACACTATTCTCAGAATGACTTGTTGAG  
TACTCACCAGTCACAGAAAAGCATCTTACGGATGGCATGACAGTAAGAGAATTATGCAGTG  
CTGCCATAACCATGAGTGATAACACTGCGGCCAACTTACTTCTGACAACGATCGGAGGACC  
GAAGGAGCTAACCGCTTTTTTGACAACATGGGGGATCATGTAACCTCGCCTTGATCGTTGG

AATCCGGAGCTGAATGAAGCCATACCAAACGACGAGCGTGACACCACGATGCCTGTAGCA  
 ATGGCAACAACGTTGCGCAAACCTATTAAGTGGCGAACTACTTACTCTAGCTTCCCGGCAAC  
 AATTAATAGACTGGATGGAGGCGGATAAAGTTGCAGGACCACTTCTGCGCTCGGCCCTTC  
 CGGCTGGCTGGTTTATTGCTGATAAATCTGGAGCCGGTGAGCGTGGGTCTCGCGGTATCA  
 TTGCAGCACTGGGGCCAGATGGTAAGCCCTCCCGTATCGTAGTTATCTACACGACGGGGA  
 GTCAGGCAACTATGGATGAACGAAATAGACAGATCGCTGAGATAGGTGCCTCACTGATTAA  
 GCATTGGGCTCTAGTACCAAGAGGCAGCTCAGAAGAGGATCTGAATAGCGCCGTCGACCA  
 TCATCATCATCAT

### 5.3 Protein Sequence of TEM-1 E166N $\beta$ -Lactamase

(Key: Cyan = Signal Peptide (removed *in situ*); Green = His-tag; Red = Thrombin cleavage site; Pink = E166N mutation)

MGSQHFRVALIPFFAAFCPLPVFAHPETLVKVKDAEDQLGARVGYIELDLNSGKILESFRPEERFP  
 MMSTFKVLLCGAVLSRVDAGQEQLGRRIHYSQNDLVEYSPVTEKHLTDGMTVRELCSAAITMS  
 DNTAANLLLTIGGPKELTAFLHNMGDHSVTRLDRWNPELNEAIPNDERDTTMPVAMATTLRKLL  
 TGELLTLASRQQLIDWMEADKVAGPLLRSALPAGWFIADKSGAGERGSRGIIAALGPDGKPSRI  
 VVIYTTGSQATMDERNRQIAEIGASLIKHWALLVPRGSSSEEDLNSAVDHHHHHH

### 5.4 Protein Expression and Purification of TEM-1 E166N $\beta$ -Lactamase

The pBAD-TEM-1-E166N plasmid was transformed into One Shot TOP10 Chemically Competent *E. coli* cells (Thermo-Fisher) using selection with 15  $\mu$ g/mL Tetracycline HCl on Luria Broth (Fisher) agar plates. A single-colony of transformed cells was grown into 5 mL overnight cultures using Terrific Broth (Fisher) with 15  $\mu$ g/mL Tetracycline HCl at 37C. Overnight cultures were then inoculated into 1 L of Terrific Broth (Fisher) media with 10  $\mu$ g/mL Tetracycline HCl shaking at 200 rpm and 37C until they reached an OD600 ~ 0.6 at which point they were induced with 2 g per L of L-(+)-Arabinose (Sigma), and grown for 4-5 hrs at 27C. Cells were harvested by centrifugation at 6000x g's for 30 mins and resuspended in lysis buffer (50mM potassium phosphate, 20mM imidazole, 500mM sodium chloride, 10% (v/v) glycerol, pH 7.4). Cells were lysed by homogenization, and the lysate centrifuged twice for 90 mins each at 15,000x g's before sterile filtering the supernatant. The crude protein was then purified using a Ni-NTA affinity resin column, washing with 50mM potassium phosphate (pH 7.4), 50mM imidazole, 500mM sodium chloride and eluted using 50mM potassium phosphate (pH 7.4), 200mM imidazole, 500mM sodium chloride. Further purification was performed using anion exchange chromatography on a 5 mL HiTrap-Q HP (GE Healthcare) column and eluted using a 0-40% gradient of Buffer A (25mM Tris (pH 8.4) 25mM sodium chloride) to Buffer B (25mM Tris (pH 8.4) 1M sodium chloride) over 25 column volumes. Purified protein was exchanged into a cryoprotectant-containing storage buffer (50 mM KPi (pH 7.4), 100 mM NaCl, 10% (v/v) glycerol) for long-term storage at -80C.

### 5.5 FTIR Spectroscopy of $^{12}\text{C}/^{13}\text{C}$ PenG, CTX, and the PenG-Acylated TEM-1 E166N $\beta$ -Lactamase

Both  $^{12}\text{C}$ - and  $^{13}\text{C}$ -PenG and CTX were prepared identically, with final lyophilized salts from HPLC being resuspended in the same  $\text{D}_2\text{O}$  buffer and lyophilized to allow H/D exchange. Before FTIR measurements were performed, lyophilized salts were resuspended in pure  $\text{D}_2\text{O}$  to a final concentration of ca. 10-25 mM. Characteristic features of these  $\beta$ -lactam antibiotics appear in the mid-IR spectral range of  $1800\text{--}1600\text{ cm}^{-1}$ , and features below  $1600\text{ cm}^{-1}$  are not considered due to spectral overlap with vibrational modes from water, protein, salts, etc. For other FTIR instrumentation details see above (Section 1.5).

In order to measure the  $^{12}\text{C} - ^{13}\text{C}$  difference spectrum, TEM-1 E166N was concentrated to ca. 2.5 mM in the storage buffer mentioned above (Section 5.3). Concentrated protein was then exchanged into a  $\text{D}_2\text{O}$  buffer (50 mM  $\text{KPi}$ , 100 mM  $\text{NaCl}$ , pD 7.0) using a Micro Bio-Spin P-6 Gel Column (BioRad), diluted 10-fold, purged with argon, and allowed to undergo H/D exchange overnight at 4-6°C. The following day, the deuterium-exchanged sample was concentrated and exchanged into a fresh  $\text{D}_2\text{O}$  buffer (same as above) for a final concentration of ca. 2.5 mM. All  $\text{D}_2\text{O}$  buffers were produced from a 10x-stock of 500 mM  $\text{KPi}$ , 1 M  $\text{NaCl}$ , pH 7.0 solution that was then lyophilized and resuspended in pure  $\text{D}_2\text{O}$  (100% atom D, Acros Organics), lyophilized, and this process repeated three times, before aliquoting into 5 mL  $\text{D}_2\text{O}$  buffer aliquots. Single-use aliquots were resuspended in pure  $\text{D}_2\text{O}$  on the intended day of use and when possible were flushed with argon to minimize H/D-exchange.

In order to obtain IR spectra of the acyl-enzyme complex (EA), the protein and either  $^{12}\text{C}$  or  $^{13}\text{C}$ -PenG were mixed to a final concentration ca. 2.7 mM PenG: 2.2 mM TEM-1 and loaded into a pre-assembled sample holder as discussed above in section 1.5. This process was repeated for both isotopes on the same day using the same protein preparation to ensure minimal difference between the two measurements.

Final isotope-edited difference spectra were generated through the following process. First, the  $^{13}\text{C}$ -PenG was scaled and subtracted from the  $^{12}\text{C}$  to remove the protein absorption. Residual unbound  $^{12}\text{C}$ - and  $^{13}\text{C}$ -PenG was subtracted from the difference spectra using the PenG  $\text{D}_2\text{O}$  buffer reference spectra. Finally, based on 2<sup>nd</sup>-derivative analysis and the  $^{12}\text{C} - ^{13}\text{C}$  PenG frequency shift of  $\sim 45\text{ cm}^{-1}$ , sets of peaks (a positive and a negative feature) were identified and baselined conservatively. This process was repeated for multiple difference spectra and baselined spectra were averaged ( $n=5$ ) to generate the spectrum presented in Figure 2D. The spectra arising from the labeled beta-lactam carbonyl group are quite complicated, consisting of a major fraction at  $1715.0\text{ cm}^{-1}$  and 2 minor fractions at  $1688.1$  and  $1654.9\text{ cm}^{-1}$ . The analysis of these spectra and their changes as a function of TEM-1 evolution towards extended-spectrum antibiotic resistance will be discussed in detail in a separate publication.

### **5.6 NMR Spectroscopy of PenG and TEM-1 E166N $\beta$ -Lactamase**

Analogous to the measurements performed above with FTIR, TEM-1 E166N was concentrated and exchanged into a  $\text{D}_2\text{O}$  buffer (50 mM  $\text{KPi}$ , 100 mM  $\text{NaCl}$ , pD 7.0) using a 10 kDa spin filter (Amicon Ultra – 4 mL). Protein was concentrated and mixed with  $^{13}\text{C}_{\text{CO}}$ -PenG in order to achieve a final concentration of ca. 0.7 mM protein and 0.5 mM PenG in 0.5 mL of the



same D<sub>2</sub>O buffer. The solution containing the acyl-enzyme complex was then pipetted into an NMR tube and spectra acquired according to the details above in section 1.5.

## **6. Appendix: Additional Information**

### **6.1 Penicillin G Production with WIS 54-1255**

#### **6.1.1 Solid Media for Sporulation**

Power medium agar<sup>[4]</sup> (pH 6.75) contains the following in g/L: 25 sucrose, 5 lactose monohydrate, 2.5 peptone, 0.5 corn steep solids, 52 potassium chloride, 1 sodium nitrate, 0.25 dibasic potassium phosphate, 0.03 monobasic potassium phosphate, 0.275 magnesium sulfate heptahydrate, 2 sodium chloride, 0.0005 copper (II) sulfate pentahydrate, 0.0015 iron (III) chloride hexahydrate, 20 agar.

Malt extract agar (ATCC medium 325; Blakeslee's formula) contains the following in g/L: 20 malt extract, 20 D-glucose, 1 peptone, 20 agar.

Sugar beet syrup agar (Figure S11; generally used for preparation of freeze-dried rice stocks) contains the following in g/L: 5 yeast extract, 7.5 mL sugar beet syrup (Grafshafter Goldsaft original sugar beet syrup), 7 mL of 85% (v/v) glycerol, 0.05 magnesium sulfate heptahydrate, 18 sodium chloride, 0.25 calcium sulfate dihydrate, 0.06 monobasic potassium phosphate, 0.01 copper (II) sulfate pentahydrate, 0.16 ammonium iron (III) sulfate dodecahydrate, 15 agar.



*Figure S11. Sugar beet agar plate after approximately 5 days exhibiting sporulation of WIS 54-1255.*

#### **6.1.2 PenG Producing Starter and Production Media Combinations**

Using any source of spores (green/blue morphology evident), penicillin G could be produced on the following tested combinations. Spore sources tested herein include sporulating Sugar Beet Agar plates, Malt Extract Agar, Power Medium, or freeze-dried rice. Combinations of starter media and penicillin production media that result in HPLC-verified penicillin G production are presented below in Table S4.

*Table S4. Media combinations with confirmed penicillin G production.*

<b>Starter Media</b>	<b>Penicillin Production Media</b>
YGG <sup>[6]</sup>	PPM+
YGG	MDFP <sup>[5]</sup>
YGG	PPM <sup>[6]</sup>
DI <sup>[5, 18]</sup>	MDFP

### **6.1.3 PenG Non-Producing Starter and Production Media Combination**

The following combinations of starter and penicillin production media as presented below in Table S5 were not shown to produce significant amounts of penicillin G (less than 100 µg per 50 mL).

*Table S5. Media combinations that produced no detectable penicillin G.*

<b>Starter Media</b>	<b>Penicillin Production Media</b>
YGG	PPM
YGG	PPM (plus citric acid)
CI <sup>[4]</sup>	PPM

### **6.1.4 <sup>15</sup>N-Incorporation Media Formulation**

Nitrogen-depleted media for general <sup>15</sup>N-incorporation, referred to as PPM+(N) (pH 6.3) contained in g/L (Table S6): 75 lactose monohydrate, 5 glucose, 10 citric acid, 5 sodium acetate, 5 ammonium sulfate (<sup>14</sup>N or <sup>15</sup>N), 3 ethylammonium chloride (<sup>14</sup>N or <sup>15</sup>N), 2.12 dibasic potassium phosphate, 5.1 monobasic potassium phosphate, 2.5 phenylacetic acid, and 10 mL of 100x Trace Elements A solution is identical to that used in SI section 2.3. Unless otherwise noted, all other protocols for media and handling are identical to that of PPM+ and PPM+(S).

*Table S6. PPM+(N) Media Formulation for <sup>15</sup>N-Incorporation.*

<b>Production Media</b>	<b>Chemical</b>	<b>g/L</b>	<b>mg/50mL</b>
<b>PPM+ (N)</b>	Glucose	5	250
pH 6.3	Lactose monohydrate	75	3750
	Ethylammonium chloride	3	150



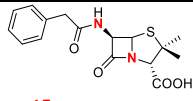
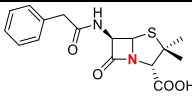
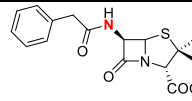
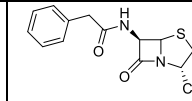
	Citric Acid	10	500
	(NH <sub>4</sub> ) <sub>2</sub> SO <sub>4</sub>	5	250
	Sodium Acetate	5	250
	K <sub>2</sub> HPO <sub>4</sub>	2.12	106
	KH <sub>2</sub> PO <sub>4</sub>	5.1	255
	Phenylacetic acid	2.5	125
	Trace Elements A (pH 6.3)	10mL	0.5mL

### 6.1.5 <sup>15</sup>N-Isotopic Enrichment: LC-MS and FTIR spectra

Using the PPM+(N) media formulation above (section 1.3), we observe that <sup>15</sup>N-incorporation into PenG can also be achieved for global incorporation.

Using the LC-MS fragmentation pattern of PenG isolated with PPM+(N) using <sup>15</sup>N incorporated from either ammonium sulfate and/or ethylammonium chloride resulted in labelling pattern shown below in Table S7. Other labelling schemes for site-specific incorporation may be feasible with further optimization of N-sources and precursor introduction into chemically defined media (e.g. <sup>15</sup>N-(L)-valine). Globally incorporated <sup>15</sup>N<sub>2</sub>-PenG was observed to have a minimal effect on the β-lactam C=O frequency (ca. 0.5 cm<sup>-1</sup>; Figure S12), limiting its application for isotope-edited FTIR difference spectra, in contrast to that shown in Figure 2.

Table S7. Site-specificity of <sup>15</sup>N-incorporation in penicillin G. Nitrogens indicated in red indicate incorporation positions of <sup>15</sup>N isotopes.

PPM+(N) <sup>15</sup> N-Sources:	 <sup>15</sup> N <sub>2</sub> -PenG	 <sup>15</sup> N <sub>1</sub> -PenG	 <sup>15</sup> N <sub>1</sub> -PenG	 <sup>14</sup> N-PenG
( <sup>15</sup> NH <sub>4</sub> ) <sub>2</sub> SO <sub>4</sub>	~50%	~20%	~20%	~10%
( <sup>15</sup> NH <sub>4</sub> ) <sub>2</sub> SO <sub>4</sub> & ( <sup>15</sup> N) Ethylammonium chloride	~100%			

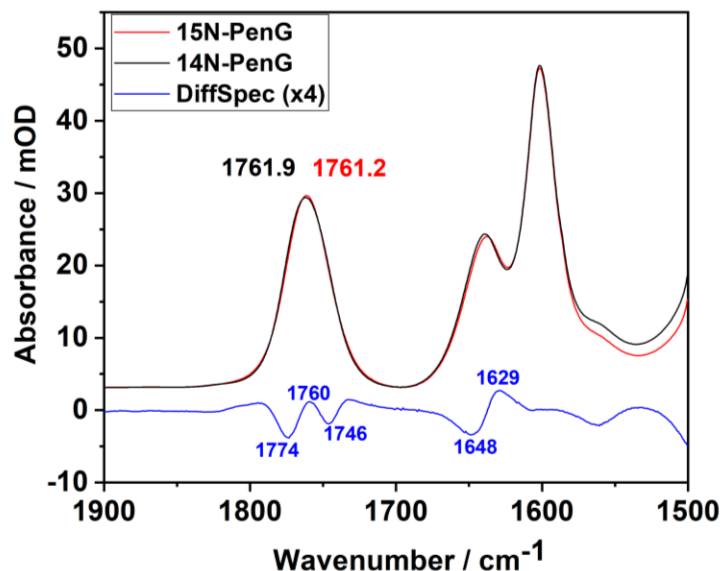


Figure S12. FTIR spectra of  $^{15}\text{N}$  and  $^{14}\text{N}$ -penicillin G in aqueous buffer (50 mM  $\text{KPi}$ , 100 mM  $\text{NaCl}$ ,  $\text{pD}$  7.0). The bottom spectrum shows the  $^{14}\text{N} - ^{15}\text{N}$  isotope-edited difference spectrum, which was enhanced by a factor of 4 to appreciate the small difference peaks.

## 6.2 Cephalosporin C Production with CW-19

### 6.2.1 Solid Media for Sporulation

SWD Medium<sup>[8]</sup> contains the following in g/L: 20 sucrose, 4 yeast extract, 4 peptone, 3 sodium nitrate, 0.5 dibasic potassium phosphate, 0.5 monobasic potassium phosphate, 0.5 potassium chloride, 0.5 magnesium sulfate heptahydrate, 0.01 iron (II) sulfate heptahydrate, 20 agar.

LPE Medium<sup>[19]</sup> contains the following in g/L (Figure S13): 10 glucose, 0.5 L-asparagine, 0.5 dibasic potassium phosphate, 18 agar.

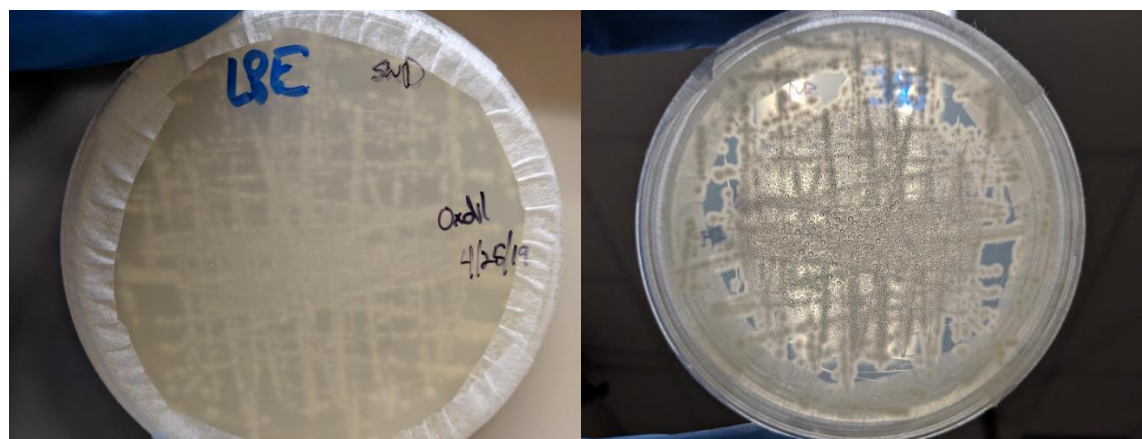


Figure S13. LPE Medium: (Left) bottom-view, (Right) front-view (with back illumination).

Malt extract agar (ATCC medium 324) contains the following in g/L: 20.0 malt extract, 5.0 peptone, 15.0 agar (Figure S14).



Figure S14. Malt extract agar: (Left) bottom-view, (middle) front-view (without back-illumination), (right) front-view (with back-illumination).

### 6.2.2 Isolation of CW-19 from ATCC 36225 Sample for CPC Production

As mentioned above in SI section 1.3, the procured samples of ATCC 36225 were sent with an additional contaminant of some unknown organism that was found to outcompete CW-19 on all solid and liquid media used herein. CPC-producing colonies of CW-19 were isolated through continuous serial dilution of sporulating agar plates until single colonies could be observed and isolated (Figure S15). After this process, no further contamination of the solid media was observed (Figure S16, right) and the contaminant strain (Figure S16, left) was found not to produce CPC by HPLC analysis. Spores from individually isolated and propagated CW-19 colonies, which were used in this study to successfully produce CPC, were provided to ATCC. Note that several studies have noted and isolated multiple morphologies in *Acremonium chrysogenum* with varying CPC production.<sup>[11-12]</sup>



Figure S15. Serial dilution of ATCC 36225 yields unique colonies on SWD agar plate. Two different morphologies are observed on the plate, one exhibits a diffuse large yellow hyphae, and the other grows in a much smaller radius with vertical growth out from the plate. Single colonies of each type were picked and re-plated on new SWD plates (see Figure S16 below).

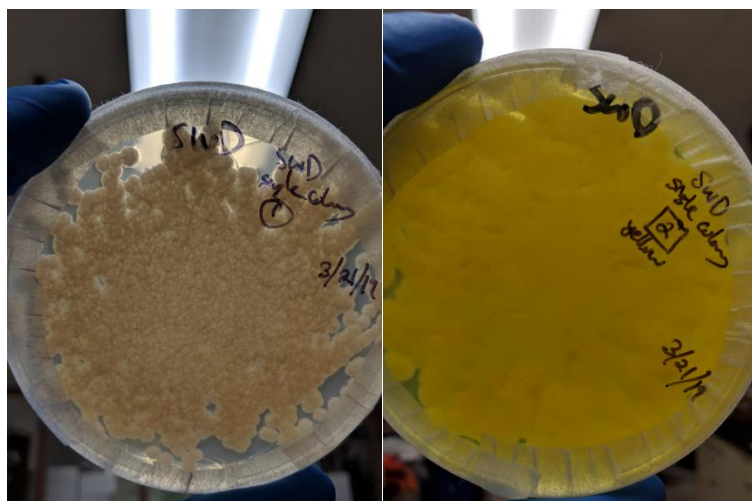


Figure S16. Re-plated single colony isolates from original ATCC 36225 sample. (Left) beige/white colonies found on solid media with propagation of ATCC 36225, which does not produce CPC using literature methods. (Right) yellow colonies exhibiting extended lateral hyphae growth on the plate and characteristic yellow coloration of colonies and underlying agar. The yellow plates were found to produce CPC and thus assumed to be CW-19, based on previous descriptions.

## 7. References:

- [1] R. P. Elander, *Appl. Microbiol. Biotechnol.* **2003**, 61, 385-392.
- [2] M.-S. Jami, C. Barreiro, C. García-Estrada, M. Juan-Francisco, *Mol. Cell. Proteom.* **2010**, 9, 1182-1198.
- [3] A. H. S. Onions, B. L. Brady, in *Penicillium and Acremonium*, Vol. 1 (Ed.: J. F. Peberdy), Springer, Boston, MA, **1987**, pp. 1-36.
- [4] M. Fernández-Aguado, R. V. Ullán, F. Teixeira, R. Rodríguez-Castro, J. F. Martín, *Appl. Microbiol. Biotechnol.* **2013**, 97, 3073-3084.
- [5] R. Domínguez-Santos, K. Kosalková, C. García-Estrada, C. Barreiro, A. Ibáñez, A. Morales, J. F. Martín, *J. Proteomics* **2017**, 156, 52-62.
- [6] S. S. Weber, F. Polli, R. Boer, R. A. Bovenberg, A. J. Driessen, *Appl. Environ. Microbiol.* **2012**, 78, 7107-7113.
- [7] L. A. Yamamoto, I. H. Segel, *Arch. Biochem. Biophys.* **1966**, 114, 523-538.
- [8] Y. Shen, S. Wolfe, A. L. Demain, *Nat. Biotechnol.* **1986**, 4, 61-64.
- [9] A. C. López-Calleja, T. Cuadra, J. Barrios-González, F. Fierro, F. J. Fernández, *J. Mol. Microbiol. Biotechnol.* **2012**, 22, 126-134.
- [10] J. F. Martín, A. L. Demain, *Trends Biotechnol.* **2002**, 20, 502-507.
- [11] S. W. Queener, L. F. Ellis, *Can. J. Microbiol.* **1975**, 21, 1981-1996.
- [12] L. T. Chang, R. P. Elander, *Develop. Ind. Microbiol.* **1979**, 20, 367-379.
- [13] J. C. Rodríguez, R. Hernández, M. González, M. A. López, A. Fini, *Il Farmaco* **2000**, 55, 393-396.
- [14] X. Ma, S. Deng, E. Su, D. Wei, *Biochem. Eng.* **2015**, 95, 1-8.
- [15] L. Pollegioni, E. Rosini, G. Molla, *Appl. Microbiol. Biotechnol.* **2013**, 97, 2341-2355.
- [16] L. Pollegioni, S. Lorenzi, E. Rosini, G. L. Marcone, G. Molla, R. Verga, W. Cabri, M. S. Pilone, *Protein Sci.* **2005**, 14, 3064-3076.

- [17] M. J. Frisch, G. W. Trucks, H. B. Schlegel, G. E. Scuseria, M. A. Robb, J. R. Cheeseman, G. Scalmani, V. Barone, G. A. Petersson, H. Nakatsuji, X. Li, M. Caricato, A. V. Marenich, J. Bloino, B. G. Janesko, R. Gomperts, B. Mennucci, H. P. Hratchian, J. V. Ortiz, A. F. Izmaylov, J. L. Sonnenberg, D. Williams-Young, F. Ding, F. Lipparini, F. Egidi, J. Goings, B. Peng, A. Petrone, T. Henderson, D. Ranasinghe, V. G. Zakrzewski, J. Gao, N. Rega, G. Zheng, W. Liang, M. Hada, M. Ehara, K. Toyota, R. Fukuda, J. Hasegawa, M. Ishida, T. Nakajima, Y. Honda, O. Kitao, H. Nakai, T. Vreven, K. Throssell, J. A. Montgomery, Jr., J. E. Peralta, F. Ogliaro, M. J. Bearpark, J. J. Heyd, E. N. Brothers, K. N. Kudin, V. N. Staroverov, T. A. Keith, R. Kobayashi, J. Normand, K. Raghavachari, A. P. Rendell, J. C. Burant, S. S. Iyengar, J. Tomasi, M. Cossi, J. M. Millam, M. Klene, C. Adamo, R. Cammi, J. W. Ochterski, R. L. Martin, K. Morokuma, O. Farkas, J. B. Foresman, D. J. Fox, Gaussian 09, Rev E.01, Gaussian, Inc., Wallingford, CT, **2016**.
- [18] J. Casqueiro, S. Gutiérrez, O. Bañuelos, M. J. Hijarrubia, J. F. Martín, *J. Bacteriol.* **1999**, *181*, 1181-1188.
- [19] G. A. LePage, E. Campbell, *J. Biol. Chem.* **1946**, *162*, 163-171.